Preprints.org

Article

Not peer-reviewed version

Morphological Reconstruction of a Critical Size Bone Defect in the Maxillofacial Region Using Modified Chitosan in Rats with sub-Compensated Type I Diabetes Mellitus

Igor N Bolshakov *, Nadezhda N. Patlataya, Vladimir A. Khorzhevskii, Anatoli A. Levenets, Nadezhda N Medvedeva, Mariya A Cherkashina, Matvey M. Nikolaenko, Ekaterina I Ryaboshapko, Anna E. Dmitrienko

Posted Date: 16 August 2023

doi: 10.20944/preprints202308.1140.v1

Keywords: modified chitosan; polyelectrolyte complex CH-SA-HA; rats; type I diabetes mellitus; bone critical size cavity; morphological reconstruction; histomorphometric criteria

Preprints.org is a free multidiscipline platform providing preprint service that is dedicated to making early versions of research outputs permanently available and citable. Preprints posted at Preprints.org appear in Web of Science, Crossref, Google Scholar, Scilit, Europe PMC.

Copyright: This is an open access article distributed under the Creative Commons Attribution License which permits unrestricted use, distribution, and reproduction in any medium, provided the original work is properly cited.

Preprints (www.preprints.org) | NOT PEER-REVIEWED | Posted: 16 August 2023 doi:10.20944/preprints202308.1140.v1

Disclaimer/Publisher's Note: The statements, opinions, and data contained in all publications are solely those of the individual author(s) and contributor(s) and not of MDPI and/or the editor(s). MDPI and/or the editor(s) disclaim responsibility for any injury to people or property resulting from any ideas, methods, instructions, or products referred to in the content.

Article

Morphological Reconstruction of a Critical Size Bone Defect in the Maxillofacial Region Using Modified Chitosan in Rats with sub-Compensated Type I Diabetes Mellitus

Nadezhda N. Patlataya [1], Igor N. Bolshakov [2]*, Vladimir A. Khorzhevskii [3] Anatolii A. Levenets [2], Nadezhda N. Medvedeva [2], Mariya A. Cherkashina [2], Matvey M. Nikolaenko [4], Ekaterina I. Ryaboshapko [2] and Anna E. Dmitrienko [2]

[1] Assistant Professor of the Department of Fundamental Medical Disciplines, Institute of Medicine and Biology, Faculty of Medicine, State Educational Institution of Higher Education, Moscow Region, Moscow State Regional University, nadya_barahtenko@mail.ru; +7 9081444547, Russia
[2] Professor of the Department Operative Surgery and Topographic Anatomy Professor V.F. Voino-Yasenetsky Krasnoyarsk State Medical University, bol.bol@mail.ru; +7 913 511 0933, Russia
[3] Head of Pathology Department, Assistant Professor, Krasnoyarsk Clinical Regional Hospital, +7 (960) 758 4040, Russia
[2] Professor of the Department Surgical Dentistry and Maxillofacial Surgery Professor V F Voino-Yasenetsky Krasnoyarsk State Medical University, aalevenets@mail.ru; +7 (902) 947 22 32; +7 (391) 220 15 70, Russia
[2] Professor of the Department of human Anatomy Professor V.F. Voino-Yasenetsky Krasnoyarsk State Medical University, medvenad@mail.ru; +7 923 276 6388, Russia
[2] Medical Student, Professor V.F. Voino-Yasenetsky Krasnoyarsk State Medical University, +7 (983) 505 12 85, Russia
[4] Resident of the Department of Maxillofacial and Plastic Surgery, A.I.Yevdokimov Moscow State University of Medicine and Dentistry, Moscow, kopm980@mail.ru; +7 (902) 957 01 98, Russia
[2] Dentistry Student, Professor V.F. Voino-Yasenetsky Krasnoyarsk State Medical University, e.ryaboshapko@yandex.ru; +7 983 1442624, Russia
[2] Dentistry Student, Professor V.F. Voino-Yasenetsky Krasnoyarsk State Medical University, Anna.E.Dmitrienko@gmail.com; +7 (913) 575 63 79, Russia University: Professor V.F. Voino-Yasenetsky Krasnoyarsk State Medical University, Russia Address: Russia, Krasnoyarsk Territory, Krasnoyarsk, 660022 st. Partisan Zheleznyak, 1 Tel No: +7 (391) 228-08-76 - Department of Affairs; +7 (391) 220-13-95 - Rector's office E-mail id: Fax: +7 (391) 2280860 Official website: krasgmu.ru E-mail: rector@krasgmu.ru
* Correspondence: bol.bol@mail.ru; Tel.: +8-913-511-0933

Abstract: It is known that complexes based on natural polysaccharides are able to eliminate bone defects. Prolonged hyperglycemia means low bone regeneration and a chronic inflammatory response. The purpose of the study was to increase the efficiency of early bone formation in a cavity of critical size in diabetes mellitus in the experiment. The polyelectrolyte complex contains high molecular ascorbate of chitosan, chondroitin sulfate, sodium hyaluronate, heparin, adgelon serum growth factor, sodium alginate and amorphous nanohydroxyapatite (CH-SA-HA). Studies were conducted on 5 groups of white female Wistar rats: group 1 - regeneration of a bone defect in healthy animals under a blood clot; group 2 - regeneration of a bone defect under a blood clot in animals with diabetes mellitus; group 3 - bone regeneration in animals with diabetes mellitus after filling the bone cavity with a collagen sponge; group 4 - filling of a bone defect with a CH-SA-HA construct in healthy animals; Group 5 - filling of a bone defect CH-SA-HA in animals with diabetes mellitus. Implantation of the CH-SA-HA construct into bone cavities in type I diabetic rats can accelerate the rate of bone tissue repair. The inclusion of modifying polysaccharides and apatite agents in the construction may be a prospect for further improvement of the properties of implants.

Keywords: modified chitosan; polyelectrolyte complex CH-SA-HA; rats; type I diabetes mellitus; bone critical size cavity; morphological reconstruction; histomorphometric criteria

© 2023 by the author(s). Distributed under a Creative Commons CC BY license.

Preprints (www.preprints.org) | NOT PEER-REVIEWED | Posted: 16 August 2023 doi:10.20944/preprints202308.1140.v1

1. Introduction

Polycationic polysaccharide polymer chitosan creates a solid frame of wound coating, enters into physical synthesis with natural anionic polymers, provides antibacterial and antitoxic effects in bone cavity, is a building material and regulator of the formation of highly organized regeneration of connective tissue, non-toxic, highly biocompatible material, completely biodegrades in the wound cavity with the transition to gel mass. Sodium alginate is a polyanionic polysaccharide polymer, forms a strong electrostatic (physical) structure with chitosan, biodegrades, is non-toxic, highly compatible with biological tissues, is a building material for bone wound regeneration, creates chemical equilibrium when included in the composition of medicinal products, increases the elasticity of the polymer structure.

In the presence of a modified chitosan polyelectrolyte complex, early signs of angiogenesis and the formation of a new bone are recorded, starting from 7 days after the experimental formation of a bone defect [1]. Filling of an extensive bone cavity with chitosan ascorbate-alginate sodium-hydroxyapatite (CH-SA-HA) containing quaternized chitosan (CH), sodium salt of alginic acid (SA) and nano-structured hydroxyapatite (HA) showed that by the end of the 4th week, 80% closure of the defect was recorded on the tomogram, and after 8 weeks - 100%. 10 weeks after the injury, there are no signs of a bone defect. The analysis registers dense bone corresponding to the density of healthy bone. The bone density in the experimental group was 810-1050 HU for the spongy substance, for the compact part - 1300-1500 HU, which is higher than in the control group.

It is known that with prolonged hyperglycemia, low bone regeneration and inflammatory response are caused by excessive formation of reactive oxygen species (ROS) and the formation of active cytokine expression with the growth of tumor necrosis factor (TNF), IL-1ß, IL-6 and IL-18 [2–5]. Lack of insulin, hyperglycemia, accumulation of glycation end products (AGE) support systemic chronic inflammation with microvascular damage. The combination of these factors violates the architecture and biomechanical properties of bone [6,7], changes the ratio of the main mineral component of hydroxyapatite and the organic component – collagen type I [8]. Overproduction of peroxides means differentiation and proliferation of osteoclasts [9–11]. Deactivation of catalase increases the concentration of H2O2 in osteoclasts, reduces the expression of antioxidant enzymes and repeatedly accelerates the differentiation, survival of osteoclasts and their proliferation [12]. On the contrary, bone resorption is accompanied by apoptosis of osteoblasts [13–15], a decrease in their differentiation and activity [16–18]. Such pathophysiological shifts in periodontal tissues weaken the girder structure of mineralized bone [6,19–21]. The initial formation of coarse fibrous connective tissue undergoes lysis as a result of collagenolytic activity of fibroblasts [22]. The prolonged inflammatory process in diabetes mellitus is accompanied by the accumulation of glycated products that cross-stitch collagen fibers in both the trabecular and cortical bones [23]. This process to deterioration of the mechanical properties of the bone [24], significantly complicates bone regeneration, especially in the presence of a bone cavity of critical size. Morphological analysis indicates the destruction of the alveolar bone in the periapical and furcal regions, an increase in the areas of accumulation of osteoclasts with signs of bone lysis [25].

A characteristic morphological sign of reduced bone regeneration is a decrease in the thickness of the bone trabecula against the background of a drop in the level of osteoblast marker – osteocalcin [26,27], alkaline phosphatase (alkaline phosphatase) and insulin-like growth factor (IGF-1). The rate of reduction of the bone callus in which cartilage is formed, the rate of cartilage resorption in the bone defect [28], the size of the newly formed bone [29] and the rate of formation of the vascular network [30] should be considered as important morphological signs of the state of bone regeneration in the analysis of the defect, requiring calculation in morphometric analysis. Hypertrophy of adipocytes in the bone marrow, a decrease in their perfusion and filling of the bone marrow with adipose tissue are morphological signs of the mesenchymal germ switching from osteoblast production to adipocyte production [31,32].

Natural polysaccharides as chitosan and sodium alginate are considered promising materials for closing the bone cavity of critical size today. These materials are the best when used for bone regeneration [33–37]. The similarity of the molecular structure of chitosan, sodium alginate,

Preprints (www.preprints.org) | NOT PEER-REVIEWED | Posted: 16 August 2023 doi:10.20944/preprints202308.1140.v1

chondroitin and hyaluronic acids, heparin sulfate, mutual improvement of their own biological properties in relation to tissue regeneration dictates the need to create copolymers with high regenerative capacity [38].

The high molecular weight of the polymer and the high positive charge reduce the degradation rate of the matrix base, which is sufficient to eliminate the bone cavity of critical size. The molecular and functional similarity with highly hydrated glycosaminoglycans (GAG) of connective tissue, the ability of anionic chemical groups (SO3, COOH-, OH-) to quaternize the chitosan molecule and collapse it to nanoscale, thereby increasing the penetrating ability through the tissue compartment, gives reason to use a polyelectrolyte chitosan complex to eliminate a bone cavity of critical size [1.39]. A very small size of the polyelectrolyte complex enhances platelet adhesion, which stimulates the functions of osteogenic cells [40], good contact of the polymer gel with the newly formed and maternal bone [41]. This reconstruction of chitosan can activate the proliferation of vascular endothelium, endothelization of the walls of the bone cavity and the polysaccharide structure itself, trigger proliferation and differentiation of osteoblasts. The task when using a biodegradable three-dimensional frame is to maintain the function and control the degradation of the polymer in the bone tissue until the full formation of a new bone. To stimulate bone neoplasm in diabetes mellitus and increase tissue strength, it is recommended to include hydroxyapatites in the complex [42–44]. Nano-sized hydroxyapatite, that ensures the strength of bone tissue, is located between bundles of collagen fibers in the form of parallel oriented plates and increases the synthesis of its own bone tissue. The inclusion of hydroxyapatite in the chitosan matrix is designed not only to enhance the strength characteristics of the implant, but also for the early formation of native bone [45].

The inclusion of angiogenic and osteogenic growth factors in the chitosan matrix accelerates the formation of a full-fledged bone. For example, preliminary studies have shown that the addition of the low-molecular-weight serum growth factor "adhelon" to the collagen-chitosan structure increases the inclusion of 3H-thymidine in the primary culture of proliferating mouse fibroblasts cultured on various substrates for 16 hours [46].

The end result of molecular transformations is a decrease in the induction of osteoclastogenesis molecules with a decrease in bone lysis zones and an increase in the volume of newly formed bone surrounding polysaccharide implants.

The inclusion of alginate and hydroxyapatite in chitosan stimulates the growth of angiogenesis factors (VEGF, CD31) in osteoblast precursors and mature osteoblasts against the background of an increase in the amount of collagen in the newly formed bone. The result of molecular transformations is the active differentiation of osteoblast precursors, the formation of a large mass of osteocytes filling a bone defect of critical size, microvascular endotheliocytes in the Havers channels [1]. For the hydration of chitosan molecules and the survival of osteoblasts, ascorbic acid is also included [47].

The concept of the study is based on the ability to form an early osteogenic reaction in the maxillofacial region using modified polysaccharides, despite the active development of diabetes mellitus and the presence of a critical size bone defect.

Thus, to confirm the formation of conditions for intensive formation of young bone in diabetes mellitus, early covering of bone beams with a mass of osteoblasts, the formation of havers channels with a high content of endotheliocytes, the authors of the work used a polyelectrolyte complex based on quaternized high-molecular chitosan with an additional degree of amination and a degree of deacetylation of 95%. The interest is a detailed morphological analysis of the bone cavity under the conditions of filling using a polysaccharide design.

2. Materials and Methods

The work was performed following ethical principles established by the European Convention for the Protection of Vertebrate Animals used for Experimental and Other Scientific Purposes (Strasbourg, 18 March 1986, adopted on 15 June 2006). All manipulations with the animals were performed following the regulations specified in the Guide for the Care and Use of Laboratory Animals (National Research Council, 2011). The work was approved: complex scientific theme No. 01201362513 (2013/01/01 – 2021/01/01) "Fundamental and applied scientific and technical

Preprints (www.preprints.org) | NOT PEER-REVIEWED | Posted: 16 August 2023 doi:10.20944/preprints202308.1140.v1

developments of nano-level biopolymer structures and technologies for their production for use in cell and tissue engineering in socially significant human diseases"; Section "Dentistry": Obtaining, testing and introduction into clinical practice of cell substrates for direct implantation into hard and soft tissues of the periodontium in order to reconstruct the tissues of the maxillofacial region, eliminate the causes of the formation of degeneration zones and the formation of periodontolysis zones; Research topic: "Restoration of the structure of the bone tissue of the maxillofacial region using polysaccharide polymers with extensive traumatic defects in conditions of sub-compensated diabetes mellitus." Bioethical Commission for Working with Animals by the Ethics Committee of the Voino-Yasenetsky Krasnoyarsk State Medical University of the Ministry of Health Russian Federation (Protocol No2 of 10/28/2019).

2.1. Composition and production of modified chitosan

Gel mass "CS-SA-HA" containing 2% solution of chitosan ascorbate (CS) (dissolution of the polymer in ascorbic solution acid in a ratio of 1: 1.5) with a molecular weight of 695 kDa and a degree of deacetylation of 95% (a special purified chitosan obtained in Vostok -Bor-1, Dal'negorsk, Russia; Specifications (No 9289-067-004721224-97), including, per 1 g of dry chitosan ascorbate, 100 mg of sodium chondroitin sulfate (Sigma), 100 mg of sodium hyaluronate (Sigma), 2,5-5 mg of heparin sulfate (Russia, Pharm.Art. (No 42-1327-99), 110 mcg \ g serum growth factors in cattle "adgelon" (SLL "Endo-Pharm-A", Moscow region, Schcholkovo, Russia, Specifications (No 113910- 001-01897475-97), 4% sodium alginate (SA) (Pharm.Art. No 42-3383-97 or Specifications (No 15-544-83; Arkhangelsk algal plant. Co), including 50% amorphous hydroxyapatite (HA) (5-20 nm, Russia, Pharm.Art. (No 42-3790- 99 or GOST 12.1.007-76), in the ratio of chitosan ascorbate and sodium alginate 1:1 [48].

7.2 grams of chitosan is added to the prepared solution of ascorbic acid (Pharm.Art. No 42-2668-95) with stirring at a temperature of + 20-25 °C, the mass is stirred for 4-5 hours until the chitosan is completely dissolved. Aqueous solutions of sodium salts of chondroitin sulfuric acid, hyaluronic acid, and heparin are successively add equal volumes to the resulting 4% chitosan solution with constant slow stirring using a magnetic stirrer in a total volume equal to the volume of chitosan ascorbate. The introduction of each subsequent ingredient is carried out only after homogeneous mixing of the previous one with the chitosan gel. As a result, 2% chitosan polyionic complex is obtained. Next, 4% aqueous solution (gel) of sodium alginate is prepared, 50% (by dry weight) of hydroxyapatite is added. The finished chitosan solution is thoroughly mixed with the sodium alginate solution using a high-speed mixer [49].

The gel mass is spillt into 2 ml vials, placed in a LZ-45 Frigera (Czech Republic) sublimation unit) at a plate temperature of +20 5 C. The mixture is frozen to a temperature of -40 3 C. Freezing time is 3-4 hours, then the chamber is put under vacuum to a residual pressure of 133 Pa (1 mm Hg), after which the process of drying the product begins due to the supply of heat from the coolant to the frozen product through heating plate surface. The sublimation process is carried out at a residual pressure of 44.3 to 133 Pa (0.33 to 1 mm Hg) and a coolant temperature of 45 5 C. The temperature of the product should not exceed +50 C. The complete drying cycle of the product is 8 2 hours. Vials with lyophilized mass are hermetically sealed and gamma sterilization is carried out at a radiation dose of 5-7 kGy.

2.2. Animal characterization and modeling of type I diabetes mellitus in rats

For the study, white female Wistar rats (supplier LLC BioTech, Moscow, weight 250 g, age 3 months at the beginning of the experiment) were used. The studies included 5 groups of animals, 10 rats in each group: group 1 (control No.1, healthy animals, comparative analysis, regeneration of the bone cavity under a blood clot); group 2 (control No.2, animals with a model of sub-compensated diabetes mellitus, regeneration of the bone cavity under a blood clot); group 3 (control No.3, animals with a model of sub-compensated diabetes mellitus, regeneration of the bone cavity when filling a bone defect with a lyophilized collagen sponge, type-I polymer, product purity 99%; "Bioactive collagen", SLL "LAONA LAB" certificate of conformity No.POCC RU.PK 08. H00305; Technical

Preprints (www.preprints.org) | NOT PEER-REVIEWED | Posted: 16 August 2023 doi:10.20944/preprints202308.1140.v1

conditions 10.11.60-001-64516066-2017; Test reports No.D0317m dated 11.28.2017; No.D0516 dated 11.28.2017 (Joint-Stock Scientific Society "Perfumetest" testing center); group 4 (control No.4, healthy animals, regeneration of the bone cavity when filling with lyophilized CH-SA-HA mass); group 5 (experienced group, animals with a model of sub-compensated diabetes mellitus, regeneration of the bone cavity during filling of a bone defect with a lyophilized mass of CH-SA-HA [1]. In each group, during morphological analysis, peripheral zones remote from the bone cavity were identified and a comparative analysis of bone regeneration in the central and peripheral zones was performed.

Destruction of pancreatic beta cells was achieved with a single subcutaneous injection of pure alloxan hydrate ($C_4H_2O_4N_2 \cdot 3H_2O$; Mm 196.17, Chemapol, Praha) at a dose of 35 mg/rat against a preliminary 48 hour fast.

Peripheral blood sugar levels were determined using an EasyTouch GCHb (Netherlands) glucometer. The period of observation of animals after the development of type I diabetes mellitus was 30 days. After the steady development of the state of hyperglycemia for 10 days at a peripheral blood sugar level above 10 mmol/l, after modeling, daily subcutaneous insulin administration at a dose of 2 ME was added (Biosulin P soluble human genetically engineered; Open Joint Stock Company Pharmstandard-UfaVITA, Russia).

2.3. The conditions of animal detention

The conditions of biological test systems in the CDI CI correspond to Guide for the Care and Use of Laboratory Animals, 8th edition, 2011, NRC, USA. The managing of animals in individually ventilated cells from polysulfone Sealsafe, 461×274×228 mm (production TECHNIPLAST.P. A.). The rooms, which contain biological test systems, controlled temperature (18-24ºC), humidity (30-70%), illumination (12/12 h), the multiplicity of air (XII without recirculation). Control of climatic parameters is carried out in accordance with the SOP "control of climatic parameters in the premises of the vivarium." Distribution of feed and water is carried out at a fixed time, the change of litter is once a week in accordance with the SOP "preparation of cells for biological test systems. Marking. Change of bedding, feed, water".

2.4. Modeling defects of the critical size in rats

Under general intramuscular anesthesia with a mixture of Zoletil 100 at a dose of 3 mg/rat and Rometar at a dose of 0.5 mg/rat, under aseptic conditions, the skin in the lower jaw was treated with an alcohol solution of chlorhexidine, an incision was made in the inferior alveolar process region, 1.5-2 cm long, The masseter muscle was bluntly separated along with the periosteum, the bone was exposed in the angle area (Figure 1). On the alveolar process, using a drill and a spherical bur, a rounded three-walled defect 4x5x4 mm in size was created (Figure 1). During surgical intervention the bone was “cooled” with an aqueous solution of chlorhexidine using boron. The cavity of the bone defect was drained with tampons and filled with CH-SA-HA lyophilic mass, collagen sponge or auto-blood clot. The defect was closed with periosteum, the skin was sutured with separate 5.0 monofilament sutures. The wound was treated with an alcohol chlorhexidine solution.

Preprints (www.preprints.org) | NOT PEER-REVIEWED | Posted: 16 August 2023 doi:10.20944/preprints202308.1140.v1

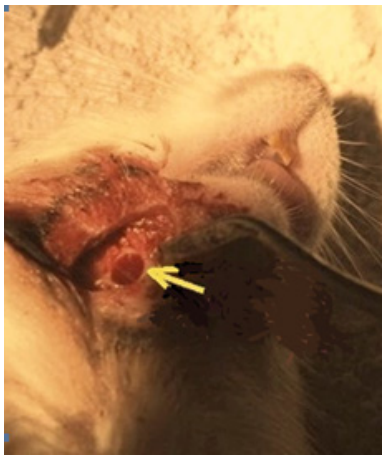

Figure 1. Drawing a defect on the rat mandible bone.

2.5. Postoperative period

Within 3 days after the intervention, the animals received Tramadol anesthetic solution 0.2 mg 2 times daily. During the first 24 hours, animals were admitted to water. Feeding was performed 24 hours after the intervention solely with a mixture of "Polyproten-nephro" based on Supra-760 protein, USA) (SLL "Protenpharma", Russia) for 3 days. Drug support was provided with a broad-spectrum antibiotic (ceftriaxone at a dose of 8 mg/rat). Animals were kept in a postoperative room with ultraviolet air sterilization and forced fine cleaning system circulation. The skin sutures were removed on the 7th day after the intervention.

2.6. Morphological analysis of bone tissue

The lower jaws were subjected to decalcification in a solution based on the disodium salt of ethylene-diamine-tetra-acetic acid (EDTA) until completely softened. The composition of the decalcifying solution: 250 g of EDTA was used per 1000 ml of distilled water with the addition of 50 ml of 40% sodium hydroxide solution. For the manufacture of histological preparations, blocks were cut out from the lower jaws of rats containing the area of a postoperative bone defect. The preparations after dehydration in ascending concentrations of alcohols were embedded in paraffin blocks. Using a MicroTec CUT4050 microtome, serial sections (20-25 sections) were made in the transverse plane (relative to the animal's body) through the entire area of the bone defect. In addition, 2-3 cuts were made along the periphery of the bone defect. The prepared sections with a thickness of 4-5 μm were stained with hematoxylin-eosin (H-E). The sectioning procedure is shown schematically (Figure 2).

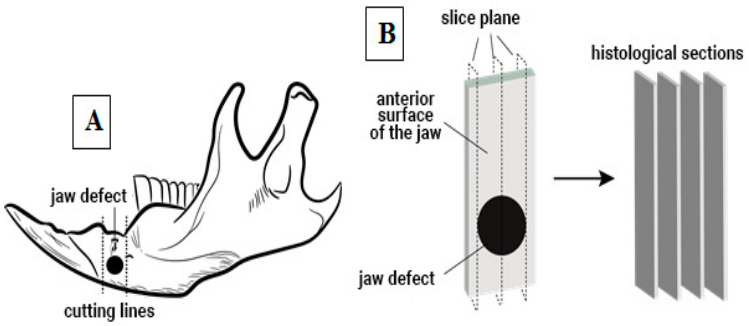

Figure 2. The procedure of the removal of fragments of the lower jaw of rats in the area of a postoperative bone defect and the preparation of histological sections. A - a fragment of the jaw after decalcification in the area of the postoperative defect was excised along the indicated incision lines; B

Preprints (www.preprints.org) | NOT PEER-REVIEWED | Posted: 16 August 2023 doi:10.20944/preprints202308.1140.v1

- the bone fragment, after being embedded in paraffin blocks, was sectioned on a microtome (as shown in Figure 2, 24-28 sections were made for each fragment).

The morphological study was carried out on an Olympus BX45 microscope with an Olympus DP 25 attachment for photo-video documentation and the Cell^D software package, as well as with scanning histological preparations in a FLASH 250 3D HISTECH histoscanner (Hungary). Plain microscopy was performed in direct and polarized light of the area of the postoperative bone defect and the peripheral zone with an assessment of the histoarchitectonics of the bone tissue. A semi-quantitative assessment was performed to determine the nature of the distribution of foreign material in the bone cavity, the cellular reaction was studied, as well as the state of the soft tissue component. Histomorphometric evaluation was performed on digital micrographs, which were obtained using the software "Cell^D" and "NIS-Elements Document", while morphometric measurements were performed in the program "JMicroVision 1.2.7". Digital histological sections obtained as a result of scanning micropreparations in a histoscanner were evaluated using the CaseViewer Ver.2.3 Build 2.3.9.99276 3D HISTECH software (Hungary).

For an objective histological assessment of bone tissue repair, criteria with a standardized nomenclature were used [49]:

- BV - volumetric density of bone tissue, the percentage ratio of the volume occupied by bone structures to the total volume of the histological section
- BTT - thickness of bone trabeculae (mm), the criterion stipulates that the bone trabecula is a thin plate, measurements were taken between the edges of the bone trabecula (5-8 measurements in relation to each trabecula with the calculation of the median)
- ITS - intertrabecular spaces (mm), the distance between the edges of the cancellous bone trabeculae, the calculation is made in accordance with the so-called parallel plate model: BV minus BTT
- OBS - osteoblastic surface of bone trabeculae, the percentage ratio of the surface of bone trabeculae occupied by osteoblasts to the total bone surface
- OS - osteoid surface of bone trabeculae, the percentage ratio of the surface of bone trabeculae occupied by osteoid to the total bone surface, was assessed by polarized light microscopy
- ES - eroded (osteoclastic) surface of bone trabeculae, the percentage ratio of the surface of bone trabeculae with the formation of gaps to the total bone surface, includes the surface occupied by osteoclasts
- TBS - total bone surface
- FS - free surface of bone trabeculae, the percentage of the non-eroded surface of bone trabeculae and the surface not occupied by osteoblasts, osteoclasts to the total bone surface

The assessment of histomorphometric parameters was performed in the area of the applied postoperative lower jaw bone defect, as well as in the area connected to the bone defect (3 mm from the edge of the bone defect). When analyzing the histomorphometric parameters of bone tissue in the periphery region of the bone defect, the authors did not divide the measurements into groups depending on the type of implanted material. Pilot studies did not show the significance of the influence of the implanted material type in the area of the bone defect on the average (median) histomorphometric values and the nature of the distribution of variable values in the peripheral area. Thus, the histomorphometric values of the peripheral area constituted an additional control group. The number of histological sections of each study group corresponded to the sensitivity (1-β) - p=0.75-0.8 (75-80%) for the estimated mean and standard deviation. The presented threshold value was chosen by taking into account the relatively small sizes of the studied samples. In this context, it should be noted that it is admissible to study small sample sizes, given that the relatively low sensitivity of such samples can be compensated for by more pronounced differences [50]. Thus, the presented acceptable sensitivity (1-β) in the used samples was compensated by a relatively low threshold value of the error of the first kind (α) – p=0.01.

2.7. Statistical analysis

Preprints (www.preprints.org) | NOT PEER-REVIEWED | Posted: 16 August 2023 doi:10.20944/preprints202308.1140.v1

Statistical analysis of data and creation of graphic illustrations were carried out using the free software computing environment "R, version 4.2.1" and the programming language "R". The assessment of the obtained variables in relation to compliance with the normal (Gaussian) distribution was carried out on the basis of the Shapiro-Wilk test, as well as on the basis of the graphical method (Quantile-Quantile plot). Most of the variables obtained obeyed the normal distribution law, and the cases of deviation of the variables from the normal distribution were not pronounced.

For variables deviating from the normal distribution, the following methods of data transformation were used to achieve compliance with the normal distribution: with right-sided (positive) skewness, square roots were taken from the obtained values, and in the case of left-sided (negative) skewness, the formula was used - $\sqrt{\mathbf{max}(x+\mathbf{1})-x}$, where "X" is the value obtained. Descriptive statistics of the obtained data were presented as median, 25% and 75% quartiles (Me[Q1;Q3]). During the choosing statistical tests for assessing the type I error (α) and the sensitivity of the criterion (1-β), parametric methods of statistical analysis were used: one-way analysis of variance (ANOVA), for paired comparisons of independent variables, Welch's t-test was used, for multiple comparisons, we used Bonferroni amendment. The presented variants of assessments were carried out taking into account the equality of variances, the variables under study, as well as taking into account the level of sensitivity of the criteria not lower than p=0.75. To assess the error of the first kind, taking into account the small volume of the studied samples, the threshold value p=0.01 was used.

3. Results

3.1. Morphological of the bone cavity walls in the induced type I diabetes mellitus development

The state of hyperglycemia in rats for 30-40 days leads to noticeable changes in the mechanisms of bone formation under conditions of regeneration of a bone cavity of a critical size. Multiple sections of bone tissue make it possible to obtain reliably distinguishable results for almost all morphometric criteria both directly in the area of surgical intervention and on the periphery of the mandible bone. The results of a low activity of osteogenesis processes are demonstrated during self-reconstruction of a bone cavity of a critical size against the background of diabetes mellitus (control 2). Characteristic signs of weak regeneration after 30 days of surgical intervention are low total bone area and trabecular thickness in combination with a wide eroded surface and multiple lacunae, poor osteoblastic reaction in combination with extensive proliferation of connective tissue and single signs of the formation of centers of bone beams. Late formation of bone trabeculae is combined with a large free surface area and low cell load (Figure 3,Table 1).

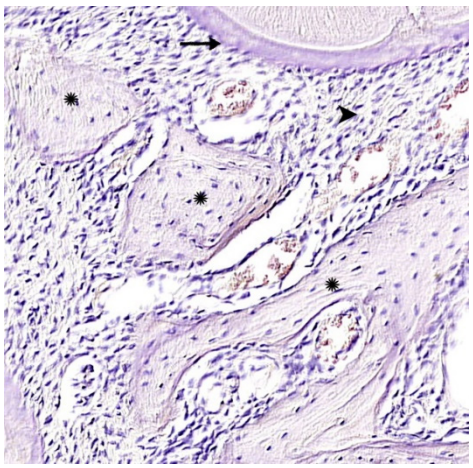

Figure 3. Control 2. Diabetes mellitus, bone cavity wall. Bone trabeculae are predominantly free surface (*) and are located among the extensive surface of the connective tissue (^), periodontal ligament (↑); Hematoxylin-eosin staining. Magnification x130.

Preprints (www.preprints.org) | NOT PEER-REVIEWED | Posted: 16 August 2023 doi:10.20944/preprints202308.1140.v1

Comparative analysis of the BV parameter of the interest zone between healthy animals (control 1) withdrawn from the experiment at week 4 and animals with sub-compensated diabetes mellitus (control 2), which showed a significant predominance of this parameter in healthy animals, both in the area of the jaw defect (in all possible variants of intergroup comparisons), and in the peripheral zone (P<0.01).

Table 1. Histomorphometric criteria for bone reconstruction in sub-compensated diabetes mellitus under CH-SA-HA implantation (Me[25;75]).

	4 weeks		Mandibular defect area				
Histomorphometric criterion	**Control 1 Healthy (under the blood clot)**	**Control 2 (diabetes mellitus) (under the blood clot)**	**Control 3 (diabetes mellitus) (collagen)**	**Control 4 Healthy (CH-SA-HA)**	**Experience (diabetes mellitus) (CH-SA-HA)**	**Peripheral zone of bone Control 4 Healthy (CH-SA-HA)**	**Peripheral zone of bone (diabetes mellitus) collagen + CH-SA-HA**
1	**2**	3	4	5	6	7	8
BV[1] (%)	60,9[58,0;62,0]**	50,4[49,5;51,3] +	56,4[55,3;57,7]***	62,9[60,7;66,8]	60,3[58,5;62,1] ✝	66,5[64,3;68,1]••	61.2[58,0;64,3]++
BTT[1] (mm)	0,14[0,13;0,15]*	0,12[0,10;0,13] +	0,13[0,12;0,15]***	0,16[0,15;0,17]	0,14[0,12;0,16] ✝	0,16[0,15;0,17] ••	0,14[0,13;0,16]++
ITS[1](mm)	0,22[0,21;0,22]**	0,20[0,19;0,21]	0,21[0,20;0,22]***	0,21[0,21;0,22]	0.20[0,19;0,21] ✝	0,21[0,20;0,22]	0,18[0,17;0,20]++
OBS[1] (%)	36,0[34,7;37,0]**	29,1[28,5;29,8] +	32,9[31,1;34,8]***	38,9[37,1;40,1]	35,5[33,4;37,5] ✝	7,2[6,3;7,8] ••	4,5[3,9;5,3]++
OS[1](%)	40,0[39,1;40,7]**	27,1[26,0;28,2] +	30,2[28,9;31,8] ***	43,3[42,8;44,3]	33,5[32,0;35,3] ✝	10,3[9,6;11,0] ••	6,9[5,9;8,0]++
ES[1](%)	10,7[10,5;11,1]**	15,4[14,2;16,6] +	11,2[10,0;12,1]***	9,9[9,7;10,0]	10,0[8,9;11,0] ✝	1,3[1,2;1,4] ••	1,3[1,1;1,4]++
FS[1](%)	53,1[52,5;54,7]**	62,0[60,3;63,7] +	56,1[54,0;57,8]***	51,5[50,1;53,2]	54,6[52,7;56,9] ✝	91,4[90,9;92,6] ••	94,1[93,4;94,8]++

* Differences are reliable with the control 4 in the area of the bone defect (p <0,05) ** Differences are reliable with the control 4 in the area of the bone defect (p <0.01) *** Differences are reliable with experience in the area of the bone defect (p <0.01) •• Differences are reliable with the corresponding variable when comparing the histomorphometric criterion of the peripheral and central zones in animals of the control group 4 (p <0.01) [1] Differences are reliable in multiple comparisons ANOVA (p <0.001) ✝ Differences are reliable when comparing the corresponding variable values in animals with diabetes mellitus control group 2 (p<0.01). + Differences are reliable with the corresponding variable in animals with diabetes mellitus of control group 2 when compared with control 4 and experience (p <0.01). ++ Differences are reliable with the corresponding variable in animals in the peripheral zone of the bone of the control group 3 and the experimental group when compared with the experimental group in the zone of the bone defect (p <0.01). BV - volumetric density of bone tissue; BTT - thickness of bone trabeculae (mm); ITS - intertrabecular spaces (mm); OBS - osteoblastic surface of bone trabeculae; OS - osteoid surface of bone trabeculae; ES - eroded (osteoclastic) surface of bone trabeculae; FS - free surface of bone trabeculae.

Comparison of the thickness of the bone trabeculae of the interest area between healthy animals and animals with sub-compensated diabetes mellitus, withdrawn from the experiment at week 4, showed significantly higher BTT values in healthy animals, both in the jaw defect area and in the peripheral zone (p<0.01). Sizes comparison of the inter-trabecular spaces of the interest area between healthy animals (control 1) and animals with sub-compensated diabetes mellitus (control 2), showed significantly lower rates of ITS in healthy animals both in the bone defect area (for all possible variants

Preprints (www.preprints.org) | NOT PEER-REVIEWED | Posted: 16 August 2023 doi:10.20944/preprints202308.1140.v1

of intergroup comparisons) and in the peripheral zone (P<0.01)). OBS in the jaws defect region of healthy rats (control 1) after 4 weeks of the experiment was significantly higher than the analogous variable with sub-compensated diabetes mellitus animals (control 2) in all possible comparisons between the available groups (P<0.01). The values of free surfaces in the peripheral zone of animals with sub-compensated diabetes mellitus were significantly higher (p<0.01) in comparison with a similar variable in the jaw defect region in healthy animals (Table 1). Thus, induced type I diabetes mellitus in rats leads, 4 weeks after the creation of a critical size bone defect, to distinct morphological disorders of osteogenesis both in the surgical intervention area and in the lower jaw peripheral zone. Such disorders are characterized by activation of the osteoclastic reaction and erosion of the bone walls, inhibition of the osteoblastic reaction during the bone trabeculae formation, and an increase in free bone surfaces depleted in cell mass of various functional directions. The presence of type I diabetes mellitus in rats contributes to a slowdown in the rate of bone tissue regeneration in the lesion compared to healthy animals.

3.2. Regeneration of the bone cavity in healthy animals when filling with CH-SA-HA

Panoramic microscopy of the bone cavity walls of a group of healthy animals 4 weeks after surgical intervention with implantation of "CH-SA-HA" was characterized by a noticeable predominance of the bone component in the formed defect area of the lower jaw, while a larger proportion of the bone beams surfaces was free from cells (Figure 4). On polarization microscopy, the bone trabeculae had a characteristic ordered and compact, fibrous structure with a typical laminar yellow-green osteoid glow (Figure 5).

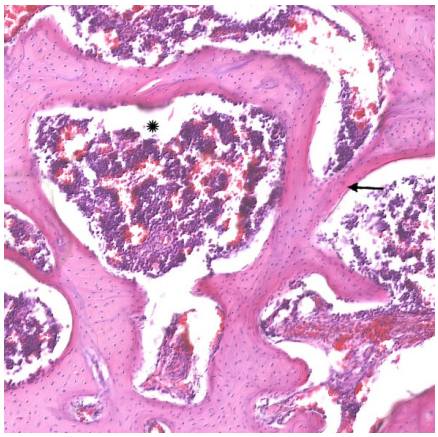

Figure 4. Control 2. Chitosan ascorbate-alginate sodium-hydroxyapatite (CH-SA-HA). Significant predominance of regenerating bone tissue in the area of the formed defect, bone beams with predominantly free surfaces (↑), reactive bone marrow structures are visible in the inter-trabecular spaces between the beams (*). Hematoxylin-eosin staining. Magnification x110.

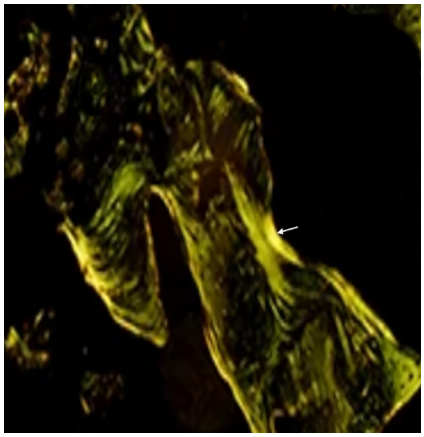

Preprints (www.preprints.org) | NOT PEER-REVIEWED | Posted: 16 August 2023 doi:10.20944/preprints202308.1140.v1

Figure 5. Control 2 "CH-SA-HA". Non-mineralized bone tissue (osteoid) in the form of surface areas with a green glow (↑). Stained with hematoxylin-eosin, polarized light. Magnification x400.

The distribution nature of the studied variable BV of bone tissue in the area of the postoperative defect and in the peripheral zone corresponded to normal, which was confirmed by the Shapiro-Wilk tests (p>0.05), as well as by visual graphic evaluation (Figure 6A).

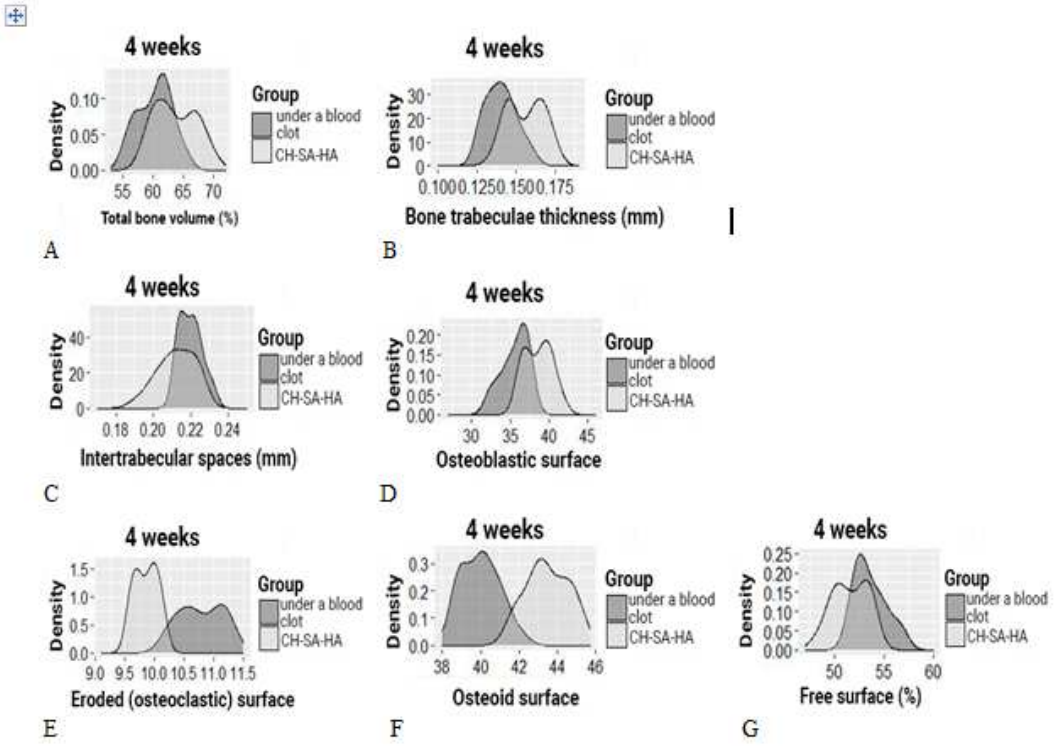

Figure 6. Histomorphometric criteria in a bone cavity of critical size in healthy rats 4 weeks after implantation of the CH-SA-HA composition: A. Distributions of the studied variable bone density (BV); B. Distributions of bone trabecula thickness (BTT) in the obtained samples; C. Variable size distributions of inter-trabecular spaces (ITSs); D. Density distribution of the OBS index in controls 1 and 2 in healthy animals after 4 weeks of observation; E. Density distribution of the eroded (osteoclastic) surface in controls 1 and 2; F. Density distribution of the osteoid surface in controls 1 and 2; G. Free surface density distribution in controls 1 and 2.

Based on one-way analysis of variance, a significant influence of the group membership factor (P<0.01) on the variable value of BV was noted. At the 4-week period, BV values in control 4 (CH-SA-HA) in the area of the postoperative defect were significantly higher (P<0.01) compared to control 1 (under the blood clot)(Figure 6A). The parameters of BV in the peripheral zone of control group 4 significantly exceeded those of control group 4 in the bone defect area with implanted bioconstruction (P<0.01)(Table 1). In the central zone of the bone defect, signs of activation of the osteoblast reaction, the formation of mature connective tissue and the structure of the cortical plate were recorded (Figure 7).

Preprints (www.preprints.org) | NOT PEER-REVIEWED | Posted: 16 August 2023 doi:10.20944/preprints202308.1140.v1

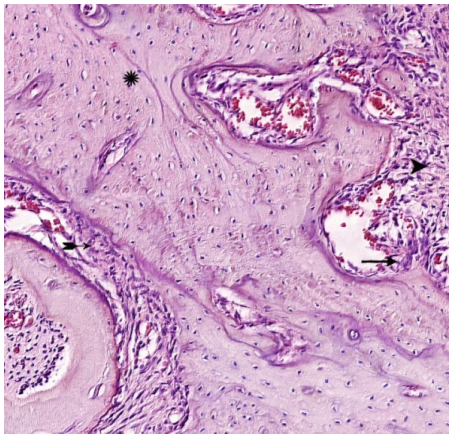

Figure 7. Morphological changes along the periphery of the bone defect in healthy rats of the CH-SA-HA group. Osteoblasts are visible in the peripheral zone (↑), maturing connective tissue (^) of the bone trabeculae structures (*) and periodontal ligament (➸) are recorded. Hematoxylin-eosin staining. Magnification x250.

The nature of the distribution of the bone trabecula thickness (BTT) in all the obtained samples corresponded to the Gaussian distribution, which was confirmed by Shapiro-Wilk tests (P>0.05), as well as visual graphical assessment (Figure 6B). Based on one-way analysis of variance, a significant effect of the group membership factor after 4 weeks of the experiment (P<0.01) on the BTT variable was noted (Table 1). Pairwise comparisons of the BTT parameters in the area of the bone defect between groups of control 1 and control 4 animals using the Welch T-test did not reveal significant differences (P>0.1). There were significant differences (P<0.01) between the BTT values of the bone defect zone and the periphery zone in control group 1 at 4 weeks.

The type of distribution of variable intertrabecular spaces (ITS) did not differ from normal, which was confirmed by Shapiro-Wilk tests (p>0.05), as well as by visual-graphic assessment (Fig. 6C). One-way statistical analysis (ANOVA) with three subgroups: controls 1 and 4 (peripheral and central zones of the bone defect) showed a significant influence (p<0.01) of the group membership factor in each experimental group. Paired comparisons between control groups 1 and 4 revealed significantly lower ITS values in the implanted biopolymer group (p<0.01). The ITS indicator in control 4 did not change when comparing the central and peripheral zones of the defect (Table 1). An analysis of the correlations connections BTT and ITS between the obtained results of an objective and histomorphometric study in the presented time interval of the experiment showed that there are no significant relationships in the control group 1 and control 4 (P>0.1). The obtained results indirectly indicate the asymmetry of the distribution of these parameters relative to each other under conditions of reparative regeneration of bone tissue. Similar results were obtained when comparing other variables (P>0.05). Histomorphometric parameters of BV, BTT and ITS, which characterize regenerative processes both in the area of the bone defect and in the peripheral zone, demonstrate variable values with opposite vectors. However, the three-dimensional picture of the distribution of these values over the 4-week period of the experiment is disordered, and no significant differences in the distribution were found.

The distribution nature of the variable OBS in all samples did not differ from normal, which was confirmed by Shapiro-Wilk tests (P>0.05). 4 weeks after filling the bone cavity with the CH-SA-HA construct (control 4), the formation of bone beams covered with multiple osteoblasts is recorded, single osteoclast cells are characteristic (Figures 8 and 9). In control 1, a reaction of active bone lysis is characteristic, a high number of osteoclasts on the bone beams (Figure 10). It should be noted that during this period in control group 4, along with the active proliferation of osteoblasts on the walls of the bone cavity (Table 1), there is simultaneously a rapid release of bone beams and the formation of intertrabecular spaces with free surfaces (Figure 11).

Preprints (www.preprints.org) | NOT PEER-REVIEWED | Posted: 16 August 2023 doi:10.20944/preprints202308.1140.v1

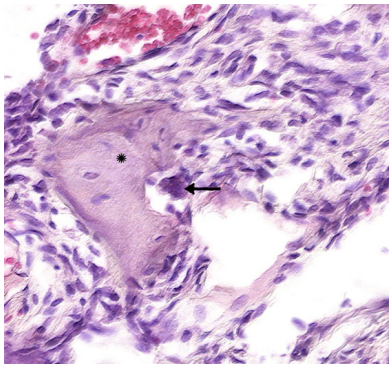

Figure 8. Control 4. CH-SA-HA. Cellular reaction in the zone of bone regeneration. Among the immature connective tissue, a bone trabecula is determined (*), an osteoclast is visible in the formed gap (↑); Hematoxylin-eosin staining. Magnification x280.

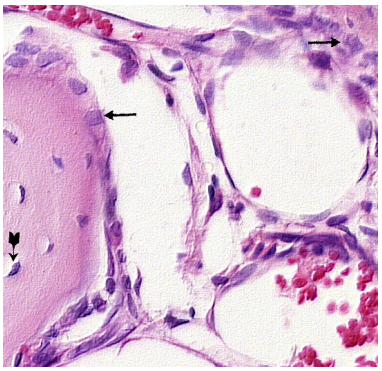

Figure 9. Control 4. CH-SA-HA design. Active annular covering of bone trabeculae by osteoblasts (↑), isolated osteocytes (➽). Hematoxylin-eosin staining. Magnification x400.

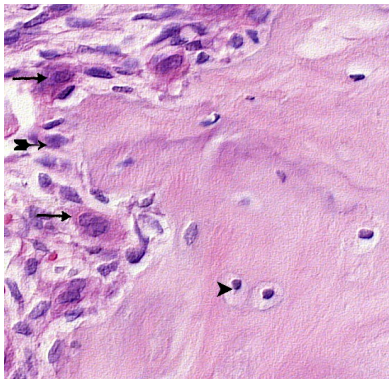

Figure 10. Control 1 (regeneration under a thrombus). Cellular reaction in the zone of bone regeneration. On the surface of the bone trabecula, an active osteoclastic reaction (↑) and a moderate number of osteoblasts (➽) are detected, in the bone tissue "isolated" osteocytes (^). Hematoxylin-eosin staining. Magnification x480.

Preprints (www.preprints.org) | NOT PEER-REVIEWED | Posted: 16 August 2023 doi:10.20944/preprints202308.1140.v1

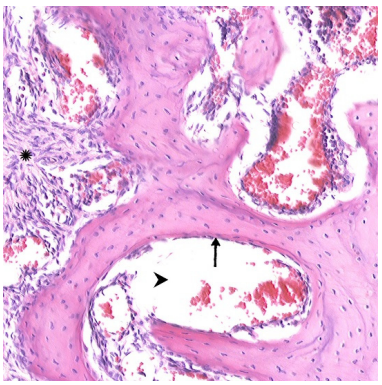

Figure 11. Control 4."CH-SA-HA design. Visible bone trabeculae with predominantly free surfaces (↑) and inter-trabecular spaces (^), adjacent peripheral area with the growth of maturing connective tissue (*). Hematoxylin-eosin staining. Magnification x130.

At 4 weeks, the OBS values in control group 4 remain higher compared to control group 1 and are 5.4 times higher than the osteoblast surface at the periphery of the bone defect (P<0.01) (Table 1). Thus, the values of the continuous variable OBS in the group with implanted biopolymer "CH-SA-HA" were significantly higher compared to both control 1 and in comparison with the peripheral zone of control group 4 animals (P<0.01)(Figure 6D).

The distribution of the histomorphometric criterion for assessing bone tissue "volume of eroded surface" (ES) in most of the formed samples did not differ from the normal one, which is shown in the graph (Figure 6E), as well as in the Shapiro-Wilk test (P> 0.05).

Pairwise comparisons using the Welch T-test 1 month after the formation of the bone cavity in control group 1 showed a significant (P<0.01) effect of the group factor on the variable value of ES. The area of bone beams of osteoclasts significantly exceeded that in the control group 4 (P<0.01). The volume of lacunar surfaces in the peripheral zone was significantly less than in the area of the bone defect (P<0.01).

The stereometric parameter of bone tissue covered with osteoid was assessed by polarizing microscopy and recorded on the basis of a homogeneous yellow-green glow on the surface of the bone beams (Figure 5). The distribution of the presented variable in all samples did not differ from normal, which is clearly demonstrated by the graphic image (Figure 6F), as well as the Shapiro-Wilk test (P> 0.05).

In pairwise comparisons between healthy control groups 1 and 4, significant differences (P<0.01) were noted at 4 weeks of follow-up, with higher values in the CH-SA-HA biopolymer implanted group. When comparing the volume of the osteoid surface of the peripheral region with the area of the bone defect with the implanted biopolymer, significantly lower values were noted in the indicated period of the experiment (Table 1).

The stereometric criterion "free surface" of bone trabeculae not occupied by osteoblasts and osteoclasts (in percent) was calculated by simply subtracting the indicators of eroded and osteoblastic surfaces from the total bone surface index. The distribution of the variable was consistent with a Gaussian distribution in all samples, as evidenced by the free surface density plot (Figure 6G) and the Shapiro-Wilk test (P>0.05). The values of the variable "free surface" with elements of descriptive statistics are shown in Table 1.

Correlation analysis between histomorphometric variables characterizing the surfaces of bone trabeculae did not show significant relationships (P>0.1).

Thus, filling a bone cavity of a critical size in the maxillofacial region with the help of the CH-SA-HA construct in healthy rats leads to the early formation of a spongy and compact bone neoformation signs. The activity of bone formation significantly exceeds the results in control group 1 in healthy animals.

3.3. Regeneration of the bone cavity walls using a collagen sponge

Preprints (www.preprints.org) | NOT PEER-REVIEWED | Posted: 16 August 2023 doi:10.20944/preprints202308.1140.v1

Implantation of a collagen sponge into the bone cavity compensates for gross violations of regeneration indicators compared to control group 2.

Bone filling with collagen sponge in rare cases, it manifests itself as a pronounced reaction from the bone marrow, which is characterized by the predominance of intermediate and mature forms of cells of the granulocytic germ. The trabecular structure of the bone cavity walls in animals with collagen sponge implantation is characterized by extensive fields of the free surface. Signs of incomplete resorption of the foreign body are characteristic among the dense and massive connective tissue (Figure 12).

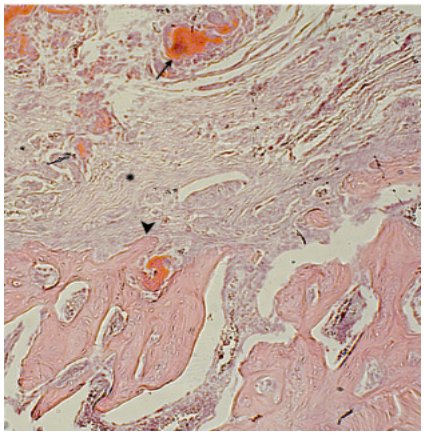

Figure 12. Control group 3 (collagen). Amphophilic structures of a foreign body (↑) are visible among dense connective tissue (*), bone trabeculae with free surfaces (^). Hematoxylin-eosin staining. Magnification x100.

However, after 4 weeks of surgical intervention in control 3, an active cellular inflammatory response persists around the collagen implant (Figure 13).

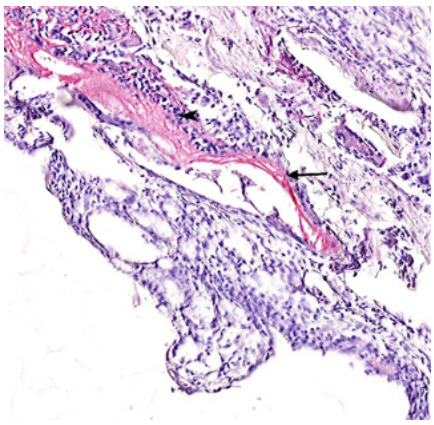

Figure 13. Control 3. Diabetes mellitus, Remains of implanted collagen (↑), cellular inflammatory infiltration around the implant (^). Hematoxylin-eosin staining. Magnification x130.

Nevertheless, implantation of a collagen sponge into a large bone cavity significantly activates new bone formation compared to the low activity in control 2. Such a high activity is manifested by the results of all evaluation criteria. Along with the high value of BV 56.4[55.3;57.7](p <0.01), the BTT and ITS values are significantly increased, especially the large area covered by osteoblasts 32.9[31.1;34.8](p <0.01) and high activity of signs formation of mature compact bone tissue – 30.2[28.9;31.8](p <0.01). At the same time, during this period of bone repair, the activity of its osteoclastic resorption was significantly reduced - 11.2[10.0;12.1](p<0.01) and the free surface volume - 56.1[54.0;57.8](p<0.01)(Table 1).

Preprints (www.preprints.org) | NOT PEER-REVIEWED | Posted: 16 August 2023 doi:10.20944/preprints202308.1140.v1

3.4. Bone defect regeneration in animals with sub-compensated diabetes mellitus under CH-SA-HA implantation

In microscopic examination of a bone defect in animals with subcompensated diabetes mellitus, signs of inflammatory infiltration in the actual walls of the defect and in the peripheral zone are usually not recorded. The histoarchitectonics of the zone of peripheral bone tissue in the animals of the study group was characterized by an ordered arrangement of bone beams with a predominance of free surfaces (Figure 14).

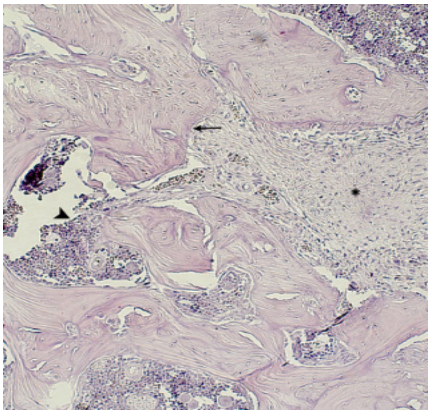

Figure 14. Regenerative changes in the bone defect and peripheral zone in rats with diabetes mellitus 30 days after construct implantation (CH-SA-HA). Bone beams with free surfaces (↑), in the field of view, a portion of the peripheral region (*) with mild infiltration by histiocytes and fibroblasts, there are reactive bone marrow structures in the inter-trabecular spaces (^). Hematoxylin-eosin staining. Magnification x100.

In the study group of animals (group 5), in the peripheral zone of the jaws was detected a pronounced reaction from the bone marrow, characterized by the predominance of intermediate and mature forms of the granulocytic germ (Figure 15).

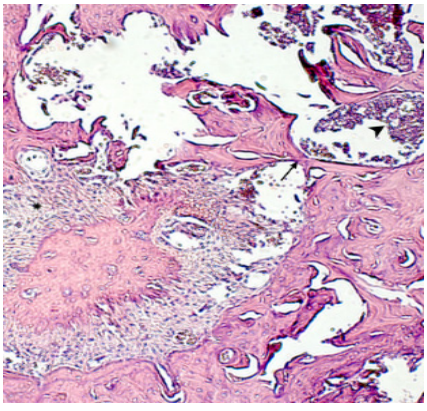

Figure 15. Animal group 5 (CH-SA-HA). In the peripheral zone, a site of maturing connective tissue is determined (*), which corresponds to the border area; mature bone tissue with unexpressed inter-trabecular spaces (↑), reactive bone marrow structures in the inter-trabecular spaces (^). Hematoxylineosin staining. Magnification x100.

In the area of the postoperative defect in the studied group of animals, there was a predominance of the bone component, represented by the structures of spongy bone (Figure 16). Bone trabeculae in the area of the postoperative defect did not have a clear spatial orientation. Most of the surfaces of the bone beams were free from cells, however, in some fields of view, flattened and cubic osteoblasts were detected on the surfaces, as well as a few osteoclasts with the formation of lacunae of varying

Preprints (www.preprints.org) | NOT PEER-REVIEWED | Posted: 16 August 2023 doi:10.20944/preprints202308.1140.v1

severity. In the area of the jaw defect, areas of bone marrow formation with a predominance of intermediate and mature forms of the granulocytic germ were revealed.

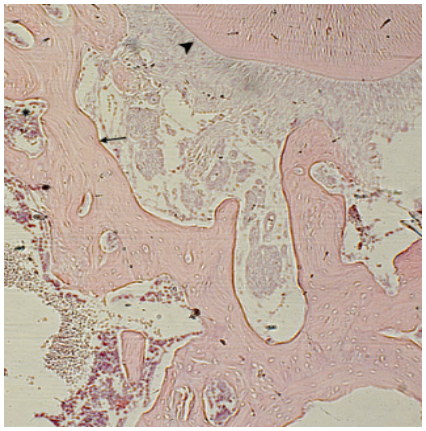

Figure 16. Study group (CH-SA-HA). Near the periodontal ligament and tooth root structures (^) a mature bone tissue (↑) with mild reactive manifestations in the bone marrow is determined (*), there are no signs of the polysaccharide structure presence (complete biodegradation). Hematoxylin-eosin staining. Magnification x100.

The results of the study show that the use of the CH-SA-HA construct in diabetes mellitus creates a high efficiency of bone regeneration and significantly compensates for the level of osteogenesis. As can be seen, in the graphic images below (Figure 17), the nature of the distribution of the obtained variables is similar to the normal distribution. One-way analysis of variance, conducted between variables with equal variances, established the significance of the group membership influence in relation to each histomorphometric variable ($p<0.01$).

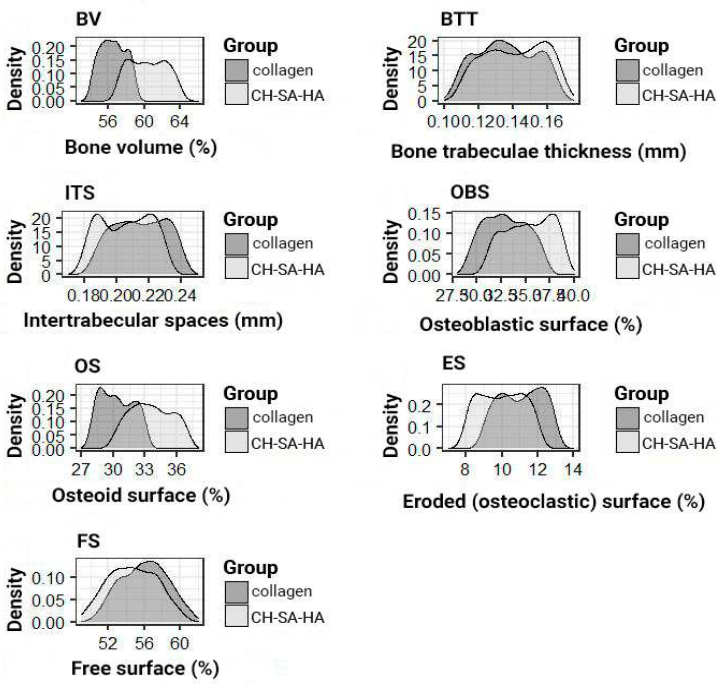

Figure 17. Density of distribution of histomorphometric parameters in the area of postoperative bone tissue defect in rats with sub-compensated diabetes mellitus in control group 3 (collagen) and the experienced group (CH-SA-HA).

Preprints (www.preprints.org) | NOT PEER-REVIEWED | Posted: 16 August 2023 doi:10.20944/preprints202308.1140.v1

The results of a comparative morphometric analysis of the bone cavity in control 3 and the experimental group of animals showed a great advantage in implantation of the proposed CH-SA-HA construct. All morphometric criteria used in this study indicate more active osteogenesis 4 weeks after surgical intervention (Table 1). When compared with the group of healthy animals (control 1), it can be stated that the process of osteogenesis compensation when using the CH-SA-HA construct in sub-compensated diabetes mellitus is at a fairly high level. It is important to note that, with the development of an active inflammatory process in the model of diabetes mellitus in rats, the peripheral zone of the bone defect (at a distance of 3 mm from the bone cavity), despite its isolation from the bone cavity and completely different numerical characteristics of bone structures, actively reacts in the form of a total decrease in the level of osteogenesis (Table 1, columns 7 and 8).

4. Conclusion

The proposed model of induced type I diabetes mellitus in rats leads, 4 weeks after the creation of a critical size bone defect, to distinct morphological disorders of osteogenesis both in the surgical intervention area and in the lower jaw peripheral zone. Such disorders are characterized by activation of the osteoclastic reaction and erosion of the bone walls, inhibition of the osteoblastic reaction during the bone trabeculae formation, and an increase in free bone surfaces depleted in cell mass of various functional directions. The presence of type I diabetes mellitus in rats contributes to a slowdown in the rate of bone tissue regeneration in the lesion compared to healthy animals, as in cases with the implanted CH-SA-HA biopolymer. Implantation of a polyelectrolyte polysaccharide complex based on modified chitosan "CH-SA-HA" in the lower jaw region of a formed critical size bone defect in healthy rats and rats with induced type I diabetes mellitus promotes a significantly faster rate of bone tissue repair. The best results of the inflammatory process resolving and restoring the bone were obtained in the absence of diabetes mellitus and cavity reconstruction using the CH-SA-HA complex as early as 4 weeks after surgical intervention. The use of a lyophilized collagen sponge based on type I collagen for the purpose of bone cavity reconstruction reliably indicates the activation of bone formation, despite the lower rates compared to the results of using the CH-SA-HA complex, and can be used in combination with modified chitosan.

5. Discussion

Significance of the obtained results in the perspective of revealing the mechanisms of osteogenesis. The results of the study showed that the dynamics of bone formation disorders under conditions of hyperglycemia during an attempt to reconstruct of a critical size bone defect in the maxillofacial region indicates the fundamental possibility of osteogenesis activation when using structures based on modified polysaccharides. It seems appropriate to address the issue of creating specialized technologies and technical means in relation to obtaining osteogenic matrices for direct transplantation into bone tissue defects. Attention should be paid to the processes of managing the start of early osteogenesis through primary early critical local angiogenesis in the maxillofacial region. The choice of the optimal carrier for the culture of osteogenic cells is one of the key stages in the creation of a tissue-engineered equivalent of bone tissue. The absence of a well-perfused module in the affected area in the early stages after extensive bone tissue trauma, the lack of the ability of synthetic materials that do not contain growth factors and osteogenic cells to cover large of a critical size bone defects [51] is one of the main problems of long-term restoration of the integrity of spongy and compact bones. The state of hyperglycemia already 4-5 weeks after the modeling of sub-compensated diabetes mellitus causes gross changes in the formation of spongy and compact bones, to a greater extent in the surgical intervention area and, to a lesser extent, on the periphery of the inflammation process.

Hyperglycemia and bone formation processes. In hyperglycemia, low bone regeneration and periodontal loss are conditioned by superoxidation (O^{-2}) in the mitochondrial electron transport chain [52–55]. The activity of membrane-bound NADPH oxidase generates high concentrations of hydrogen peroxide (H_2O_2) in organelles. It is known that the overproduction of peroxides leads through the activation of the signaling pathway of the mRNA of blood plasma: the receptor-activator

Preprints (www.preprints.org) | NOT PEER-REVIEWED | Posted: 16 August 2023 doi:10.20944/preprints202308.1140.v1

of nuclear factor-ligand-kappa-B (RANKL) to the differentiation and proliferation of osteoclasts [56–58]. An increase in the osteoclasts H^2O^2 concentration reduces the expression of antioxidant enzymes and accelerates the differentiation and survival of osteoclasts. Such events weaken the mineralized bone beams structure [59,60]. Proliferation of osteoclasts means a process of impaired ossification [61], activation of pro-apoptotic genes and osteoblast apoptosis. This leads to erosion and weakening of the bone beams [62–64]. It has been established that the development of periodontitis against the background of diabetes mellitus is accompanied by a high level of IL-1β, TNF-α, MCP-1 chemokine and prostaglandin E2, which cause and prolong osteoclast-mediated bone resorption [65].

Attention should be paid to the creation of conditions for early endothelialization of the matrix, translation of the vascular endothelium from the walls of the bone cavity into the structure. The formation of micro-vessels is the basis for the physiologically active process of bone formation [66]. So, early local angiogenesis means an early start of osteogenesis mechanisms. Tight contact of the initially cell-free copolymer matrix with spongy and compact plates of the bone cavity with a certain filling of polymers with angiogenesis products triggers the process of matrix endothelization. Thus, early endothelialization of the artificial matrix is the primary task and will mean oriented sprouting of precursors or specialized cells, as well as signaling molecules of intercellular interaction, and, as a result, an active process of early osteogenesis [67]. The present studies have shown that, despite the successful solution of the issue of early bone formation, the first stage of the process of reconstruction of the vasculature remains insufficiently understood from the point of view of the contact interaction mechanism between the vascular endothelium and artificial or natural polymers. It is known that stimulation of proliferation and translation of vascular endothelium occurs outside the vascular wall into the tissue compartment [68,69]. If polymer matrices are used, during the degradation of which nanoparticles are formed, this enhances the efficiency of vector molecules delivery to cells and leads to over expression of angiogenesis molecules, enhances endothelial recruitment and new formation of blood micro-vessels [70]. Thus, angiogenesis occurs earlier than new bone formation [71]. Using this postulate, it should be clarified that the formation of micro-vessels in the matrix body is also an earlier stage of reconstruction, followed by osteogenesis [68,72,73]. At the same time, one of the important conditions for the rapid integration of a building structure is, in addition to degradation, high biocompatibility, the manifestation of its own angiogenic qualities, the ability to block polysaccharide and protein structures on the microbial cell surface that provide transmembrane transport, and the ability to block pain conduction on somatic cells. Modern approaches to solving the problem of vascularization also include the introduction of angiogenic and osteogenic growth factors into the injury zone based on a biodegradable polymer framework, which plays the role of not only a depot for dislocation of growth factors, but also a program for their long-term elution as a result of a certain rate of polymer biodegradation. Dosed elution of growth factors from a modern polysaccharide matrix forms new capillaries [74]. The initial start of endothelialization ends with the rapid filling of the cell-free matrix with the vascular network. The osteoblastic and osteoclastic microenvironment of the vascular implant stimulates the rapid formation of spongy and compact bone from the periphery to the center of the implant. It is very important that the artificially created vascular network does not regress after the complete utilization of the implant. Uncovering the mechanisms of the initial stages of angiogenesis will solve the problem of critical early osteogenesis.

The role of collagen in the reconstruction of a bone defect in combination with polysaccharides (chitosan, alginate). As shown by the present studies, collagen is able to improve the morphological and histological characteristics of the bone in the maxillofacial region in animals with induced diabetes mellitus. However, it is known that the use of pure collagen is not designed to directly activate angiogenesis. The inclusion of chitosan in the collagen complex triggers the formation of the vascular network [75]. Additional inclusion of growth factors or other protein molecules in the framework of collagen and chitosan copolymer is used not only to implement the direct functions of signaling molecules, but also to improve the binding of properties of materials [76,77]. In connection with this conclusion, it can be assumed that the collagen-chitosan copolymer is a promising material for the reconstruction of large bone defects. The addition of a standard apatite component to the chitosan base, which is used for plasty in the maxillofacial region in patients [78,79],

Preprints (www.preprints.org) | NOT PEER-REVIEWED | Posted: 16 August 2023 doi:10.20944/preprints202308.1140.v1

as well as the use of an intermediate product of the bone apatite base, octacalcium phosphate ($Ca_8H_2(PO_4)_6 \cdot 5H_2O$), found in human dentin, is an attempt to obtain a higher activity of inclusion in the early process of bone regeneration and an improved alternative to autologous bone grafting [80]. It is fair to clarify that the same regularity is also revealed when the alginate-hydroxyapatite framework is combined with poly-lactic acid [81,82], ethyl-cellulose, and poly(Ɛ-caprolactone) [83]. In general, the introduction of additional natural polysaccharide polymers into the structure leads to obtaining not only excellent mechanical strength, but, which is very important, to the active implementation of cellular functions such as adhesion, proliferation and differentiation. For example, a composite scaffold consisting of a chitosan, alginate, hydroxyapatite combination, and cellulose nanocrystals possesses such properties, which is especially valuable for bone tissue engineering.

Attention should be paid to the use of sulfated polysaccharides, such as heparin, in the study in the preparation of the functional copolymer. Three sulfate groups in the heparin molecule allow large rigid linear polymers to be transformed into nanosized globules, which predetermines their high mobility in living animal tissues [84. It is noteworthy that along with the high specific affinity of heparin for growth factors, for example, bFGF [85], the presence of a mechanism of active electrostatic interaction between the negatively charged heparin sulfate groups and the positively charged amino acid residues of the growth factor leads to an increase in binding affinity [86]. An additional positive feature of the heparin use is the fact that its low molecular weight allows loading a large amount of polysaccharide into a large carrier molecule. An important role in the binding of heparin and growth factor is played by hydrogen bonds and van der Waals packing [87]. Such a polymer network becomes resistant to enzymatic hydrolysis. The high affinity of heparin for growth factors ensures high protein loading. The higher the growth factor loading, the higher the effect of angiogenesis. It is very important that such a technology for incorporating a growth factor with a good final functional result can be applied by conjugation of two or more polysaccharides. The heparin introduction into high-molecular scaffolds on alginate and chitosan based has good mechanical properties, non-toxicity, low immunogenicity and is able to regulate the degradation rate [88].

The role of modified chitosan in the bone cavity reconstruction. Studies have shown that modified chitosan without diabetes can significantly improve the histomorphological characteristics of the bone cavity walls in the maxillofacial region. It is known that the use of a chitosan membrane as a single polymer leads to the formation of new bone and cementum in single-wall intraosseous defects in large experimental animals [89]. The combined use of biopolymers in one structure is designed for the mutual penetration of individual polymers with the hydrogel networks formation, which creates reinforcement of the structure and is considered one of the best technologies for obtaining a composite with high mechanical properties [90]. Such reinforcement was performed in the work of Bolshakov IN et al., when type 1 collagen [91] was introduced into the modified chitosan structure. Such a structure was implanted in a mechanical complete rupture of the spinal cord in rats. The initial cell-free collagen-chitosan construct (Fig. 18A) was actively filled with inflammatory infiltrate cells and neuronal progenitors within 1-20 weeks after injury (Fig. 18B,C). Maintaining the rigidity of the scaffold and its simultaneous degradation for 20 weeks allowed the animals to maintain a viable specialized cell mass with signs (Fig. 18D) of good blood supply. Such active filling of the cell mass of collagen-chitosan construction led to almost complete restoration of the spinal cord conduction system with demonstration of motor, sensory and vegetative functions.

Preprints (www.preprints.org) | NOT PEER-REVIEWED | Posted: 16 August 2023 doi:10.20944/preprints202308.1140.v1

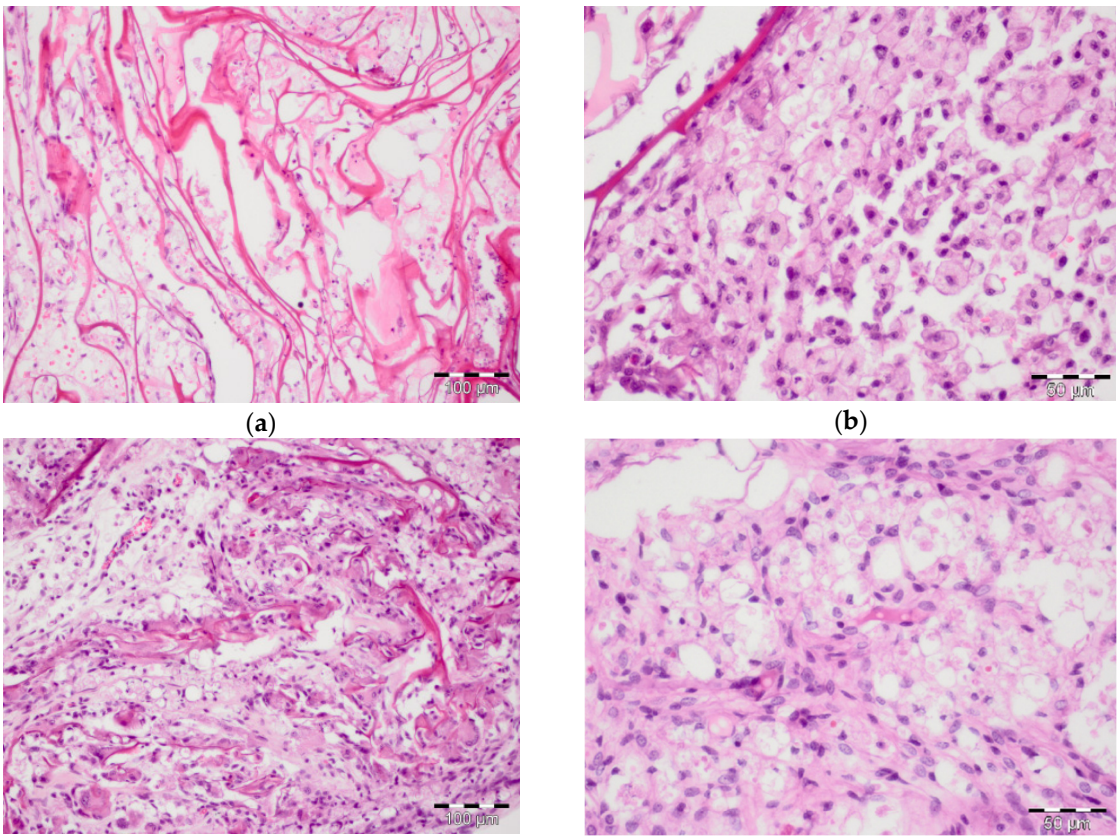

Figure 18. Fig.18A. Cell-free collagen-chitosan matrix based on modified chitosan in complete nutrient medium DMEM for 28 days. Azur-eosin stain, x100 magnification. Fig.18B. Matrix filling 7 days later with mouse neuronal progenitors (PNCm) after transplantation into a rat spinal cord defect. Macrophage infiltration with phagocytic debris. Azur-eosin staining, x200 magnification. Fig.18C. The construct in the rat spinal cord is filled with a viable cell mass of precursors of mouse neuronal cells (PNCm) and macrophages, the collagen-chitosan scaffold is preserved for 28 days. Azur-eosin stain, x100 magnification. Fig.18D. Poorly differentiated progenitors of viable neuronal cells in the matrix, 28 days after implantation. Azur-eosin staining, x200 magnification.

Similar combined meshes are known, which were used in our work, with the inclusion of alginate and chitosan [92] or hyaluronic acid [93,94] in the design for the purpose of bone tissue bioengineering. The low penetrating ability of chitosan as an independent molecule through the inflammatory tissue compartment can be significantly increased by creating a complex polyelectrolyte structure, which leads to the densification of the polymer to nanosizes. Previous experimental work on the preparation of chitosan complexes with sulfated polysaccharides showed the ability of polyelectrolyte complexes to undergo globular conformation and transform into nanosizes [84]. It has been established that, upon passing from pH 1.55 to pH 3.5, the size of nanoparticles decreases from 200-220 nm to 48-52 nm due to a pH-dependent change in the conformational state of the molecule. Most likely, in the environment of the stratified epithelium of the oral cavity, where the pH is close to 5.5, the nanometer scale of molecular sizes is a fundamental factor for the chitosan use. The design, which contains high purity and deacetylated chitosan, sodium chondroitin sulfate, sodium hyaluronate, heparin sulfate, sodium alginate, amorphous hydroxyapatite in certain weight ratios, is designed for early stimulation of bone formation. It is known that a nanosized surface, in comparison with a micro-sized one, is a stimulus for the proliferation of endothelial cells and osteogenic cells [95]. It is important to note that a high degree of deacetylation of the chitosan matrix plays an important role both in terms of structure degradation and in the degree of its endothelization [67]. An important intermediate goal when introducing a polyelectrolyte construct into a bone cavity of a critical size is to increase the efficiency of the

Preprints (www.preprints.org) | NOT PEER-REVIEWED | Posted: 16 August 2023 doi:10.20944/preprints202308.1140.v1

polysaccharide implant structures contact with the bone walls and microvascular bed of the bone in a shorter time after the intervention. The goal is achieved due to the fact that a nanogel mass of chitosan-alginate-hydroxyapatite (CH-SA-HA) is introduced into large cavities. These studies are an example of experimental modeling of the real situation of protection of "small molecules in aggressive environments, for example, the oral cavity, and is directly related to solving the problem of targeted medicinal substances' transportation fixed on chitosan.

The use of a combination of chitosan with an alginate–hydroxyapatite framework [96–99] stabilizes the gel matrix due to the formation of polyelectrolyte complexes. The complexes are formed as a result of a weak interaction of oppositely charged chemical groups of COO^- alginate and NH_3^+ of chitosan. In addition, NH_3^+ groups can interact with PO_4^{3-} hydroxyapatite groups, linking the framework together and forming a more compact structure. At the same time, porosity and degradation rate decrease, and mechanical stability increases. If we are talking about the destruction of periodontal tissues in the experiment, then the filling of a bone defect with a chitosan complex with a polyanionic structure [100] leads to inhibition of the apical migration of the epithelium and active formation of new bone and cementum. Thus, there is a need to use such constructs to close critical bone defects in diabetes mellitus, given the well-known scientific findings that reveal the mechanisms of activation of osteogenesis and angiogenesis. Biodegradable polysaccharide biopolymers as the main substrates for self-regulation, as well as for the purpose of overexpression of osteogenic and angiogenic growth factors, activation of mesenchymal stem cells, osteoblast precursors, and vascular endothelial cells can be considered as promising constructs in the treatment of a specific inflammatory process in the periodontium. Solving this problem is a complex project, since systemic impairment of bone formation in diabetes mellitus affects extracellular, transcellular, and intracellular mechanisms associated with osteoinduction and osteoconduction. The complexity of the regulation of the cytokine storm and the development of osmotic and oxidative stress in cells with the accumulation of peroxides requires the use of complex building structures for contact with the maternal bone that can interfere with the processes of osteoclast activation, bone resorption, osteomalacia, and prolonged inflammation in the periodontal zone. In this regard, polysaccharide biopolymers, such as chitosan or alginate, are very promising for bone bioengineering. They can independently or in the presence of exogenous growth factors increase the quality and volume of mineralization, the formation of bone beams with a large mass of osteoblasts and osteoids, and increase the total number of osteocytes in the newly formed bone. It has been established that in the presence of chitosan, alginate in combination with nano-hydroxyapatite in vitro and in vivo system, the growth of angiogenesis factors (VEGF, CD31) in osteoblast precursors and mature osteoblasts is detected early, the amount of collagen I in the zone of the newly formed bone with high serum bone alkaline activity phosphatase (BAP). The active proliferation of osteoblast precursors, the formation of a large mass of osteocytes filling a bone critical size defect, microvascular endotheliocytes in Haversian canals confirm the wide functional nature of modified chitosan implants in relieving the inflammatory process in induced diabetes mellitus.

Acknowledgments and project funding application: The authors express their gratitude to the staff of the Center for Collective Use of the Prof. Voyno-Yasenetsky Krasnoyarsk State Medical University Ministry of Health of the Russian Federation for providing the laboratory conditions for the physical synthesis of a polyelectrolyte complex based on natural polysaccharides and performing experimental work on animals in accordance with international requirements. The authors express their gratitude to the staff of the morphological studies laboratory of the Krasnoyarsk Federal Cancer Center for their help in obtaining, scanning histological sections and obtaining high-resolution figures (supervisor - Candidate of Medical Sciences, Associate Professor S.S. Bekuzarov (contract No. 117.20217-D dated November 17, 2017 and contract No. 120.2017-D dated December 1, 2017.). The work was approved: complex scientific theme No. 01201362513 (2013/01/01 – 2021/01/01) "Fundamental and applied scientific and technical developments of nano-level biopolymer structures and technologies for their production for use in cell and tissue engineering in socially significant human diseases"; Section "Dentistry": Obtaining, testing and introduction into clinical practice of cell substrates for direct implantation into hard and soft tissues of the periodontium in order to reconstruct the tissues of the maxillofacial region, eliminate the causes of the formation of degeneration zones and the formation of periodontolysis zones; Research topic: "Restoration of the structure of the bone tissue of the maxillofacial region using polysaccharide polymers with extensive traumatic defects in conditions of subcompensated diabetes mellitus. The

Preprints (www.preprints.org) | NOT PEER-REVIEWED | Posted: 16 August 2023 doi:10.20944/preprints202308.1140.v1

implementation of the project was consulted on the basis of the Center for Collective Use scientific base Prof. V.F. Voyno-Yasenetsky Krasnoyarsk State Medical University and the Federal Research Center "Krasnoyarsk Scientific Center of the Siberian Branch of the Russian Academy of Sciences" on the basis of agreement No. 1-2/1 of 10/23/2017 and No. 1-2/2 dated 10/23/2017 between the Regional State Autonomous Institution "Krasnoyarsk Regional Innovation and Technology Business Incubator" ("KRITBI") and FSBEI HE "Krasnoyarsk State Medical University after Prof. Voyno-Yasenetsky Ministry Health of Russia, LLC "Bioimplant" (Krasnoyarsk) (General Director Bolshakov I.N.)(the agreement No. 2/t dated 09/13/2017).

Conflicts of Interest: The authors have no conflicts of interest relevant to this article.

References

1. Bolshakov, I. N.; Levenets, A. A.; Patlataya, N. N.; Nikolaenko, M. M.; Dmitrienko, A. E.; Ryaboshapko, E. I.; Matveeva, N. D.; Ibragimov, I. G.; Kotikov, A. R.; Furtsev, T. V. The Role of Modified Chitosan in Bone Engineering in Diabetes Mellitus: Analytical Review. Int. J. Dent. Oral. Health. **2021**, 7 (3), 1-13; dx.doi.org/10.16966/2378-7090.356.
2. Yamagishi, S. Role of advanced glycation end products (AGEs) in osteoporosis in diabetes. Curr. Drug Targets. **2011,** 12 (14), 2096–3002; DOI: 10.2174/138945011798829456.
3. Graves, D. T.; Kayal, R. A. Diabetic complications and dysregulated innate immunity. NIH Public Access Author Manuscript. Front Biosci. **2008**, 13, 1227–1239; DOI: 10.2741/2757.
4. Nikolajczyk, B. S.; Jagannathan-Bogdan, M.; Shin, H.; Gyurko, R. State of the union between metabolism and the immune system in type 2 diabetes. Genes Immun. **2011**, 12 (4), 239–250; DOI: 10.1038/gene.2011.14.
5. García-Hernández, A.; Arzate, H.; Gil-Chavarría, I.; Rojo, R.; Moreno-Fierros, L. High glucose concentrations alter the biomineralization process in human osteoblastic cells. Bone. **2012**, 50 (1), 276–288; DOI: 10.1016/j.bone.2011.10.032.
6. Napoli, N.; Chandran, M.; Pierroz, D. D.; Abrahamsen, B.; Schwartz, A. V.; Ferrari, S. L. Mechanisms of diabetes mellitus-induced bone fragility. Nat. Rev. Endocrinol. **2017**, 13, 208–219; DOI: 10.1038/nrendo.2016.153.
7. Napoli, N.; Strollo, R.; Paladini, A.; Briganti, S. I.; Pozzilli, P.; Epstein, S. The alliance of mesenchymal stem cells, bone, and diabetes. Int. J. Endocrinol. **2014**, 2014, 690783; DOI: 10.1155/2014/690783.
8. Landis, W. J. The strength of a calcified tissue depends in part on the molecular structure and organization of its constituent mineral crystals in their organic matrix. Bone. **1995**, 16, 533–544; DOI: 10.1016/8756-3282(95)00076-p.
9. Lee, N. K.; Choi, Y. G.; Baik, J. Y.; Han, S. Y.; Jeong, D.-W.; Bae, Y. S.; Kim, N.; Lee, S. Y. A crucial role for reactive oxygen species in RANKL-induced osteoclast differentiation. Blood. **2005**, 106 (3), 852-859; DOI: 10.1182/blood-2004-09-3662.
10. Tanaka, S.; Nakamura, K.; Takahasi, N.; Suda, T. Role of RANKL in physiological and pathological bone resorption and therapeutics targeting the RANKL-RANK signaling system. Immunol. Rev. **2005**, 208, 30-49; DOI: 10.1111/j.0105-2896.2005.00327.x.
11. Ha, H.; Kwak, H.;B.; Lee, S.;W.; Jin, H.;M.; Kim, H.-M.; Kim, H.-H.; Lee Z. H. Reactive oxygen species mediate RANK signaling in osteoclasts. Exp. Cell Res. **2004,** 301 (2), 119-127; DOI: 10.1016/j.yexcr.2004.07.035.
12. Liu, R.; Bal, H.;S.; Desta, T.; Krothapalli, N.; Alyassi, M.; Luan, Q.; Graves, D. T. Diabetes enhances periodontal bone loss through enhanced resorption and diminished bone formation. J. Dent. Res. **2006**, 85 (6), 510–514; DOI: 10.1177/154405910608500606.
13. Andriankaja, O. M.; Galicia, J.; Dong, G.; Xiao, W.; Alawi, F.; Graves, D. T. Gene expression dynamics during diabetic periodontitis. J. Dent. Res. **2012**, 91 (12), 1160-1165; DOI: 10.1177/0022034512465292.
14. Pacios, S.; Andriankaja, O.; Kang, J; Alnammary, M.; Bae, J.; Bezerra, B. de B.; Schreiner, H.; Fine, D. H.; Graves, D. T. Bacterial infection increases periodontal bone loss in diabetic rats through enhanced apoptosis. Am. J. Pathol. **2013**, 183 (6), 1928–1935; DOI: 10.1016/j.ajpath.2013.08.017.
15. Alblowi, J.; Tian, C.; Siqueira, F. M.; Kayal, R. A.; McKenzie, E.; Behl, Y.; Gerstenfeld, L.; Einhorn, T. A.; Graves, D. T. Chemokine expression is upregulated in chondrocytes in diabetic fracture healing. Bone. **2013**, 53 (1), 294–300; DOI:10.1016/j.bone.2012.12.006.
16. Katayama, Y.; Akatsu, T.; Yamamoto, M.; Kugai, N.; Nagata, N. Role of nonenzymatic glycosylation of type I collagen in diabetic osteopenia. J. Bone Miner. Res. **1996**, 11 (7), 931-937; DOI: 10.1002/jbmr.5650110709.
17. Stolzing, A.; Sellers, D.; Llewelyn, O.; Scutt, A. Diabetes induced changes in rat mesenchymal stem cells. Cells Tissues Organs. **2010**, 191 (6), 453-465; DOI: 10.1159/000281826.
18. García-Hernández, A.; Arzate, H.; Gil-Chavarría, I.; Rojo, R.; Moreno-Fierros, L. High glucose concentrations alter the biomineralization process in human osteoblastic cells. Bone. **2012**, 50 (1), 276-288; DOI: 10.1016/j.bone.2011.10.032.
19. Bartell, S. M.; Kim, H-N.; Ambrogini, E.; Han, L.; Iyer, S.; Ucer, S.S.; Rabinovitch, P.; Jilka, R. L.; Weinstein, R. S.; Zhao, H.; O'Brien, C. A.; Manolagas, S. C.; Almeida, M. FoxO proteins restrain

Preprints (www.preprints.org) | NOT PEER-REVIEWED | Posted: 16 August 2023 doi:10.20944/preprints202308.1140.v1

osteoclastogenesis and bone resorption by attenuating H2O2 accumulation. Nat. Commun. **2014**, 5, 3773; DOI: 10.1038/ncomms4773.

20. Wang, Y.; Dong, G.; Jeon, H. H.; Elazizi, M.; La, L. B.; Hameedaldeen, A.; Xiao, E.; Tian, C.; Alsadun, S.; Choi, Y.; Graves D. T. FOXO1 mediates RANKL-induced osteoclast formation and activity. J. Immunol. **2015**, 194 (6), 2878-2887; DOI: 10.4049/jimmunol.1402211.
21. Kang, J.; de Bezerra, B. B.; Pacios, S.; Andriankaja, O.; Tsiagbe, V.; Li, Y.; Schreiner, H.; Fine, D. H.; **Graves**, D. T. Aggregatibacter actinomycetem comitans infection enhances apoptosis in vivo through a caspase-3-dependent mechanism in experimental periodontitis. Infect. Immun. **2012**, 80 (6), 2247-2256; DOI: 10.1128/IAI.06371-11.
22. Richardsand, D.; Rutherford, R. The effects of interleukin 1 on collagenolytic activity and prostaglandin-E secretion by human periodontal-ligament and gingival fibroblasts. Arch. Oral Biol. **1988**, 33, 237–243; DOI: 10.1016/0003-9969(88)90184-7.
23. Leslie, W. D.; Rubin, M. R.; Schwartz, A. V.; Kanis, J. A. Type 2 diabetes and bone. J. Bone Miner. Res. **2012**, 27, 2231–2237; DOI: 10.1002/jbmr.1759.
24. Saito, M.; Marumo, K. Collagen cross-links as a determinant of bone quality: a possible explanation for bone fragility in aging, osteoporosis, and diabetes mellitus. Osteoporos. Int. **2010**, 21, 195–214; DOI: 10.1007/s00198-009-1066-z.
25. Mahamed, D. A.; Marleau, A.; Alnaeeli, M.; Singh, B.; Zhang, X.; Penninger, J. M.; Teng, T.-Y. A. G(−) anaerobes-reactive CD4 + T-cells trigger RANKL-mediated enhanced alveolar bone loss in diabetic NOD mice. Diabetes. **2005**, 54 (5): 1477–1486; DOI: 10.2337/diabetes.54.5.1477.
26. Shetty, S.; Kapoor, N.; Bondu, J. D.; Thomas, N.; Paul, T. V. Bone turnover markers: Emerging tool in the management of osteoporosis. Indian J. Endocrinol. Metab. **2016,** 20, 846–852; DOI: 10.4103/2230-8210.192914.
27. Maggio, A. B. R.; Ferrari, S.; Kraenzlin, M.; Marchand, L. M.; Schwitzgebel, V.; Beghetti, M.; Rizzoli, R.; Farpour-Lambert, N. J. Decreased bone turnover in children and adolescents with well controlled type 1 diabetes. J. Pediatr. Endocrinol. Metab. **2010**, 23, 697–707; DOI: 10.1515/jpem.2010.23.7.697.
28. Kayal, R. A.; Tsatsas, D.; Bauer, M. A.; Allen, B.; Al-Sebaei, M. O.; Kakar, S.; Leone, C. W.; Morgan, E. F.; Gerstenfeld, L. C.; Einhorn, T. A.; Graves D. T. Diminished Bone Formation During Diabetic Fracture Healing is Related to the Premature Resorption of Cartilage Associated With Increased Osteoclast Activity. J. Bone Miner. Res. **2007**, 22 (4), 560–568; DOI: 10.1359/jbmr.070115.
29. Kayal, R. A.; Siqueira, M.; Alblowi, J.; McLean, J.; Krothapalli, N.; Faibish, D.; Einhorn, T. A.; Gerstenfeld, L. C.; Graves, D. T. TNF-alpha mediates diabetes-enhanced chondrocyte apoptosis during fracture healing and stimulates chondrocyte apoptosis through FOXO1. J. Bone Miner. Res. **2010,** 25 (7), 1604–1615; DOI: 10.1002/jbmr.59.
30. Claes, L.; Recknagel, S.; Ignatius, A. Fracture healing under healthy and inflammatory conditions. Nat.Rev. Rheumatol. **2012**, 8, 133–143; DOI: 10.1038/nrrheum.2012.1.
31. Li, Y.-M.; Shilling, T.; Benisch P.; Zeck, S.; Meissner-Weigl, J.; Schneider, D.; Limbert, C.; Seufert, J.; Kassem, M.; Schütze, N.; Jakob, F.; Ebert R. Effects of high glucose on mesenchymal stem cell proliferation and differentiation. Biochem. Biophys. Res. Commun. **2007**, 363 (1), 209-215; DOI: 10.1016/j.bbrc.2007.08.161.
32. Hamada, Y.; Fujii, H.; Fukagawa, M. Role of oxidative stress in diabetic bone disorder. Bone. **2009**, 45 (1), S35–38; DOI: 10.1016/j.bone.2009.02.004.
33. Kozusko, S. D.; Riccio, C.; Goulart, M.; Bumgardner, J.; Jing, X. L.; Konofaos, P. Chitosan as a bone scaffold biomaterial. J. Craniofacial Surg. **2018**, 29 (7), 1788-1793; DOI: 10.1097/SCS.0000000000004909.
34. Kumbhar, S. Self-functionalized, oppositely charged chitosan-alginate scaffolds for biomedical applications. BioTechnology: An Indian J. **2017**, 3 (2), 1-15.
35. Rodríguez-Vázquez, M.; Vega-Ruiz, B.; Ramos-Zúñiga, R.; Saldaña-Koppel, D. A.; Quiñones-Olvera, L. F. Chitosan and its potential use as a scaffold for tissue engineering in regenerative medicine. BioMed. Res. Int. **2015**, special iss. New biomaterials in drug delivery and wound care: article ID 821279; DOI: org/10.1155/2015/821279.
36. Jiang, T.; Kumbar, S. G.; Nair, L. S.; Laurencin, C. T. Biologically active chitosan systems for tissue engineering and regenerative medicine. Curr. Top. Med. Chem. **2008**, 8 (4), 354-364; DOI: 10.2174/156802608783790974.
37. Costa-Pinto, A. R.; Reis, R. L.; Neves, N. M. Scaffolds based bone tissue engineering: the role of chitosan. Review. Tissue Eng. Part B Rev. **2011**, 17, (5), 331-347; DOI: 10.1089/ten.teb.2010.0704.
38. Spin-Neto, R.; Coletti, F. L.; de Freitas, R. M.; Pavone, C.; Campana-Filholo, S. P.; Marcantonio, R. A. C. Chitosan-based biomaterials used in critical-size bone defects: radiographic study in rat's calvaria. Rev. Odontol. UNESP. **2012**, 41 (5), 312-317; DOI:10.1590/S1807-25772012000500003.
39. Dhandayuthapani, B.; Yoshida, Ya.; Maekawa, T.; Kumar, D. S. Polymeric scaffolds in tissue engineering application: a review. Int. J. Polymer Sci. **2011**, Article ID 290602:1-19; DOI:10.1155/2011/290602.

Preprints (www.preprints.org) | NOT PEER-REVIEWED | Posted: 16 August 2023 doi:10.20944/preprints202308.1140.v1

40. Chatzipetros, E.; Christopoulos, P.; Donta, C.; Tosios, K.-I.; Tsiambas, E.; Tsiourvas, D.; Kalogirou, E.-M.; Tsiklakis K. Application of nano-hydroxyapatite/chitosan scaffolds on rat calvarial critical-sized defects: a pilot study. Med. Oral Patol. Oral Cir. Bucal. **2018**, 23 (5), e625-632; DOI:10.4317/medoral.22455.
41. Hu, J. X.; Ran, J. B.; Chen, S.; Jiang, P.; Shen, X. Y.; Tong, H. Carboxylated agarose (CA)-silk fibroin (SF) dual confluent matrices containing oriented hydroxyapatite (HA) crystals: biomimetic organic/inorganic composites for tibia repair. Biomacromolecules. **2016**, 17 (7), 2437-2447; DOI: 10.1021/acs.biomac.6b00587.
42. Luo, Y.; Lode, A.; Wu, C.; Chang, J.; Gelinsky, M. Alginate/nanohydroxyapatite scaffolds with designed core/shell structures fabricated by 3D plotting and in situ mineralization for bone tissue engineering. ACS Appl. Mater. Interfaces. **2015**, 7 (12), 6541-6549; DOI: 10.1021/am508469h.
43. Koshihara, Y.; Kawamura, M.; Oda, H.; Higaki, S. In vitro calcification in human osteoblastic cell line derived from periosteum. Biochem. Biophys. Res. Comm. **1987**, 145, (2), 651-657; http://dx.doi.org/10.1016/0006-291X(87)91014-X.
44. Chung, T.-W.; Liu, D.-Z.; Wang, S.-Y.; Wang, S.-S. Enhancement of the growth of human endothelial cells by surface roughness at nanometer scale. Biomaterials. **2003**, 24 (25), 4655-4661; DOI: 10.1016/S0142-9612(03)00361-2.
45. Vissarionov, S. V.; Asadulaev, M. S.; Shabunin, A. S.; Yudin, V. E. Experimental evaluation of the efficiency of chitosan matrixes under conditions of modeling of a bone defect in vivo (preliminary report). Pediatric traumatology, orthopedics and reconstructive surgery. **2020**, 8 (1), 53–62; https://doi.org/10.17816/PTORS16480.
46. Patent RF 2254145, 20/06/2005.
47. Patel, Z. S.; Young, S.; Tabata, Y.; Jansen, J. A.; Wong, M. E.; Mikos, A. G. Dual delivery of an angiogenic and an osteogenic growth factor for bone regeneration in a critical size defect model. Bone. **2008**, 43 (5), 931–940; DOI: 10.1016/j.bone.2008.06.019.
48. Patent RF 2309748, 01/10/2006.
49. Dempster, D. W.; Compston, J. E.; Drezner, M. K.; Glorieux, F. H.; Kanis J. A.; Malluche, H.; Meunier, P. J.; Ott, S. M.; Recker, R. R.; Parfitt, A. M. Standardized nomenclature, symbols, and units for bone histomorphometry: a 2012 update of the report of the ASBMR Histomorphometry Nomenclature Committee. J. Bone Miner. Res. **2013**, 28 (1), 2-17; DOI: 10.1002/jbmr.1805.
50. Morgan, C. J. Use of proper statistical techniques for research studies with small samples. Am. J. Physiol. Lung Cell Mol. Physiol. **2017**, 313 (5), L873-L877; DOI:10.1152/ajplung.00238.2017.
51. Lovett, M.; Lee, K.; Edwards, A.; Kaplan D. L. Vascularization strategies for tissue engineering. Tissue Eng. Part B Rev. **2009**, 15 (3), 353–370; DOI: 10.1089/ten.TEB.2009.0085.
52. Giacco, F.; Brownlee, M. Oxidative stress and diabetic complications. Rev. Circ. Res. **2010**, 107 (9), 1058-1070; DOI: 10.1161/CIRCRESAHA.110.223545.
53. Pitocco, D.; Zaccardi, F.; Di Stasio, E.; Romitelli, F.; Santini, S. A.; Zuppi, C.; Ghirlanda, G. Oxidative stress, nitric oxide, and diabetes. Rev. Diabet. Stud. Spring. **2010**, 7 (1), 15-25; DOI: 10.1900/RDS.2010.7.15.
54. Pitocco, D.; Tesauro, M.; Alessandro, R.; Ghirlanda, G.; Cardillo, C. Oxidative stress in diabetes: implications for vascular and other complications. Int. J. Mol. Sci. **2013**, 14 (11), 21525-21550; DOI: 10.3390/ijms141121525.
55. Folli, F.; Corradi, D.; Fanti, P.; Davalli, A.; Paez, A.; Giaccari, A.; Perego, C.; Muscogiuri, G. The role of oxidative stress in the pathogenesis of type 2 diabetes mellitus micro- and macrovascular complications: avenues for a mechanistic-based therapeutic approach. Curr. Diabetes Rev. **2011**, 7 (5), 313-324; DOI: 10.2174/157339911797415585.
56. Lee, N. K.; Choi, Y. G.; Baik, J. Y.; Han, S. Y.; Jeong, D. W.; Bae, Y. S.; Kim, N.; Lee, S. Y. A crucial role for reactive oxygen species in RANKL-induced osteoclast differentiation. Blood. **2005**, 106 (3), 852-859; DOI: 10.1182/blood-2004-09-3662.
57. Tanaka, S.; Nakamura, K.; Takahasi, N.; Suda, T. Role of RANKL in physiological and pathological bone resorption and therapeutics targeting the RANKL-RANK signaling system. Immunol. Rev. **2005**, 208, 30-49; DOI: 10.1111/j.0105-2896.2005.00327.x.
58. Ha, H.; Kwak, H. B.; Lee, S. W.; Jin, H. M.; Kim, H.-M.; Kim, H.-H.; Lee, Z. H. Reactive oxygen species mediate RANK signaling in osteoclasts. Exp. Cell Res. **2004**, 301 (2), 119-127; DOI: 10.1016/j.yexcr.2004.07.035.
59. Bartell, S. M.; Kim, H.-N.; Ambrogini, E.; Han, L.; Iyer, S.; Ucer, S. S.; Rabinovitch, P.; Jilka, R. L.; Weinstein, R. S.; Zhao, H.; O'Brien, C. A.; Manolagas, S. C.; Almeida, M. FoxO proteins restrain osteoclastogenesis and bone resorption by attenuating H2O2 accumulation. Nat. Commun. **2014**, 5, 3773; DOI: 10.1038/ncomms4773.
60. Wang, Y.; Dong, G.; Jeon, H. H.; Elazizi, M.; La, L. B.; Hameedaldeen, A.; Xiao, E.; Tian, C.; Alsadun, S.; Choi, Y.; Graves, D. T. FOXO1 mediates RANKL-induced osteoclast formation and activity. J. Immunol. **2015**, 194 (6), 2878-2887; DOI: 10.4049/jimmunol.1402211.
61. Kang, J.; de Bezerra, B. B.; Pacios, S.; Andriankaja, O.; Li, Y.; Tsiagbe, V.; Schreiner, H.; Fine, D. H.; Graves, D. T. Aggregatibacter actinomycetem comitans infection enhances apoptosis in vivo through a caspase-3-

Preprints (www.preprints.org) | NOT PEER-REVIEWED | Posted: 16 August 2023 doi:10.20944/preprints202308.1140.v1

dependent mechanism in experimental periodontitis. Infect. Immun. **2012**, 80 (6), 2247-2256; DOI: 10.1128/IAI.06371-11.

62. Andriankaja, O. M.; Galicia, J.; Dong, G.; Xiao, W.; Alawi, F.; Graves, D. T. Gene expression dynamics during diabetic periodontitis. J. Dent. Res. **2012**, 91 (12), 1160-1165; DOI: 10.1177/0022034512465292.
63. Pacios, S.; Andriankaja, O.; Kang, J.; Alnammary, M.; Bae, J.; Bezerra, B. de B.; Schreiner, H.; Fine, D. H.; Graves, D. T. Bacterial infection increases periodontal bone loss in diabetic rats through enhanced apoptosis. Am. J. Pathol. **2013**, 183 (6), 1928–1935; DOI: 10.1016/j.ajpath.2013.08.017.
64. Alblowi, J.; Tian, C.; Siqueira, M. F.; Kayal, R. A.; McKenzie, E.; Behl, Y.; Louis, G.; Einhorn, T. A.; Graves, D. T. Chemokine expression is upregulated in chondrocytes in diabetic fracture healing. Bone. **2013**, 53 (1), 294–300; DOI:10.1016/j.bone.2012.12.006.
65. Alblowi, J.; Kayal, R. A.; Siqueira, M.; McKenzie, E.; Krothapalli, N.; McLean, J.; Conn, J.; Nikolajczyk, B.; Einhorn, T. A.; Gerstenfeld, L.; Graves, D. T. High levels of tumor necrosis factor-alpha contribute to accelerated loss of cartilage in diabetic fracture healing. Am. J. Pathol. **2009,** 175 (4), 1574–1585; DOI: 10.2353/ajpath.2009.090148.
66. Hasegawa, T.; Yamamoto, T.; Tsuchiya, E.; Hongo, H.; Tsuboi, K.; Kudo, A.; Abe, M.; Yoshida, T.; Nagai, T.; Khadiza, N.; Yokoyama, A.; Oda, K.; Ozawa, H.; de Freitas, P. H. L.; Li, M.; Amizuka, N. Ultrastructural and biochemical aspects of matrix vesiclemediated mineralization. Jpn. Dent. Sci. Rev. **2017**, 53 (2), 34–45; DOI: 10.1016/j.jdsr.2016.09.002.
67. Amaral, I. F.; Neiva, I.; da Silva, F. F.; Sousa, S. R.; Piloto, A. M.; Lopes, C. D. F.; Barbosa, M. A.; Kirkpatrick, C. J.; Pego, A. P. Endothelialization of chitosan porous conduits via immobilization of a recombinant fibronectin fragment (rhFNIII(7-10)). Acta Biomaterialia. **2013**, 9 (3), 5643-5652; DOI: 10.1016/j.actbio.2012.10.029.
68. Sivaraj, K. K.; Adams, R. H. Blood vessel formation and function in bone. Development. **2016**, 143 (15), 2706-2715; DOI: 10.1242/dev.136861.
69. Gorustovich, A. A.; Roether, J. A.; Boccaccini, A. R. Effect of bioactive glasses on angiogenesis: A Review of in vitro and in vivo evidences. Tissue Eng. Part B Rev. **2010**, 16 (2), 199–207; DOI: 10.1089/ten.TEB.2009.0416.
70. Thomas, A. M.; Gomez, A. J.; Palma, J. L.; Yap, W. T.; Shea, L. D. Heparin-chitosan nanoparticle functionalization of porous poly(ethylene glycol) hydrogels for localized lentivirus delivery of angiogenic factors. Biomaterials. **2014**, 35 (30), 8687-8693; DOI: 10.1016/j.biomaterials.2014.06.027.
71. Stegen, S.; van Gastel, N.; Carmeliet, G. Bringing new life to damaged bone: The importance of angiogenesis in bone repair and regeneration. Bone. **2015**, 70, 19-27; DOI: 10.1016/j.bone.2014.09.017.
72. Kuttappan, S.; Mathew, D.; Jo, J.-I.; Tanaka, R.; Menon, D.; Ishimoto, T.; Nakano, T.; Nair, S. V.; Nair, M. B.; Tabata, Y. Dual release of growth factor from nanocomposite fibrous scaffold promotes vascularisation and bone regeneration in rat critical sized calvarial defect, Acta Biomater. **2018**, 78, 36–47; DOI: 10.1016/j.actbio.2018.07.050.
73. Nguyen, L. H.; Annabi, N.; Nikkhah, M.; Bae, H.; Binan, L.; Park, S.; Kang, Y.; Yang, Y.; Khademhosseini, A. Vascularized bone tissue engineering: approaches for potential improvement, Tissue Eng. Part B Rev. **2012**, 18 (5), 363–382; DOI: 10.1089/ten.TEB.2012.0012.
74. Sheridan, M. H.; Shea, L. D.; Peters, M. C.; Mooney, D. J. Bioabsorbable polymer scaffolds for tissue engineering capable of sustained growth factor delivery. J. Control Release. **2000**, 64 (1-3), 91-102; DOI: 10.1016/s0168-3659(99)00138-8.
75. Vojtová, L.; Pavliňáková, V.; Muchová, J.; Kacvinská, K.; Brtníková, J.; Knoz, M.; Lipový, B.; Faldyna, M.; Göpfert, E.; Holoubek, J.; Pavlovský, Z.; Vícenová, M.; Blahnová, V. H.; Hearnden, V.; Filová, E. Healing and angiogenic properties of collagen/chitosan scaffolds enriched with hyperstable FGF2-STAB® protein: In vitro, ex novo and in vivo comprehensive evaluation. Biomedicines. **2021**, 9 (6), 590; https://doi.org/10.3390/biomedicines9060590.
76. Croisier, F.; Jérôme, C. Chitosan-based biomaterials for tissue engineering. Eur. Polym. J. **2013**, 49 (4), 780–792; DOI:10.1016/j.eurpolymj.2012.12.009.
77. Muchová, J.; Hearnden, V.; Michlovská, L.; Vištejnová, L.; Zavad'áková, A.; Šmerková, K.; Kočiová, S.; Adam, V.; Kopel, P.; Vojtová, L. Mutual influence of selenium nanoparticles and FGF2-STAB® on biocompatible properties of collagen/chitosan 3D scaffolds: In vitro and ex novo evaluation. J. Nanobiotechnol. **2021**, 19 (1), 103; DOI:10.1186/s12951-021-00849-w.
78. Habraken, W.; Habibovic, P.; Epple, M.; Bohner, M. Calcium phosphates in biomedical applications: Materials for the future? Materials Today. **2015**, 19 (2), 69–87; https://doi.org/10.1016/j.mattod.2015.10.008.
79. Kokubo, T.; Kim, H. M.; Kawashita, M. Novel bioactive materials with different mechanical properties. Biomaterials. **2003**, 24 (13), 2161–2175; https://doi.org/10.1016/S0142-9612(03)00044-9.
80. Kamakura, S.; Nakajo, S.; Suzuki, O.; Sasano, Y. New scaffold for recombinant human bonemorphogenetic protein-2. J. Biomed. Mater. Res. Part A. **2004**, 71 (2), 299-307; DOI:10.1002/jbm.a.30157.
81. Fernández-Cervantes, I.; Morales, M.; Agustín-Serrano, R.; Cardenas-García, M.; Pérez-Luna, P.; Arroyo-Reyes, B.; Maldonado-García, A. Polylactic acid/sodium alginate/hydroxyapatite composite scaffolds with

Preprints (www.preprints.org) | NOT PEER-REVIEWED | Posted: 16 August 2023 doi:10.20944/preprints202308.1140.v1

trabecular tissue morphology designed by a bone remodeling model using 3D printing. J. Mater. Sci. **2019**, 54 (13), 1-19; DOI:10.1007/s10853-019-03537-1

82. Hu, Y.; Ma, S.; Yang, Z.; Zhou, W.; Du, Z.; Huang, J.; Yi, H.; Wang, C. Facile fabrication of poly (L-lactic acid) microsphere-incorporated calcium alginate/hydroxyapatite porous scaffolds based on Pickering emulsion templates. Colloids Surf. B. **2016**, 140, 382–391; DOI: 10.1016/j.colsurfb.2016.01.005.
83. Hokmabad, V. R.; Davaran, S.; Aghazadeh, M.; Rahbarghazi, R.; Salehi, R.; Ramazani, A. Fabrication and characterization of novel ethyl cellulose-grafted-poly (ε-caprolactone)/alginate nanofibrous/macroporous scaffolds incorporated with nano-hydroxyapatite for bone tissue engineering. J. Biomater. Appl. **2019**, 33 (8), 1128–1144; DOI: 10.1177/0885328218822641.
84. Bolshakov, I. N.; Levenetz, A. A.; Furtsev, T. V.; Kotikov, A. R.; Patlataya, N. N.; Ryaboshapko, E. I.; Dmitrienko, A. E.; Nikolaenko, M. M.; Matveeva, N. D.; Ibragimov, I. G. Experimental Reconstruction of Critical Size Defect of Bone Tissue in the Maxillofacial Region When Using Modified Chitosan. Biomed. Transl. Sci. **2022**, 2 (1), 1-8; DOI:10.33425/2768-4911.1024.
85. Lu, Q.; Li, M.; Zou, Y.; Cao, T. Delivery of basic fibroblast growth factors from heparinized decellularized adipose tissue stimulates potent *de novo* adipogenesis. J. Control Release. **2014**, 174, 43-50; DOI: 10.1016/j.jconrel.2013.11.007.
86. Shen, H.; Hu, X.; Yang, F.; Bei, J.; Wang, S. Cell affinity for bFGF immobilized heparin-containing poly(lactide-co-glycolide) scaffolds. Biomaterials. **2011**, 32 (13), 3404-3412; DOI: 10.1016/j.biomaterials.2011.01.037.
87. Thompson, L. D.; Pantoliano, M. W.; Springer, B. A. Energetic characterization of the basic fibroblast growth factor-heparin interaction: identification of the heparin binding domain. Biochemistry. **1994**, 33, (13), 3831-3840; DOI: 10.1021/bi00179a006.
88. Hu, X. X.; Shen, H.; Yang, F.; Bei, J. Z.; Wang, S. G. Preparation and cell affinity of microtubular orientation-structured PLGA(70/30) blood vessel scaffold. Biomaterials. **2008**, 29 (21), 3128-3136; DOI: 10.1016/j.biomaterials.2008.04.010.
89. Yeo, Y. J.; Jeon, D. W.; Kim, C. S.; Choi, S. H.; Cho, K. S.; Lee, Y. K.; Kim, C.-K. Effects of chitosan nonwoven membrane on periodontal healing of surgically created one-wall intrabony defects in beagle dogs. J. Biomed. Mater. Res. B Appl. Biomater. **2005**, 72 (1), 86-93; DOI: 10.1002/jbm.b.30121.
90. Darnell, M.; Sun, J.; Mehta, M.; Johnson, C.; Arany, P. R.; Suo, Z.; Mooneyl, D. J. Performance and biocompatibility of extremely tough alginate/polyacrylamide hydrogels. Biomaterials. **2013**, 34 (33), 8042-8048; DOI: 10.1016/j.biomaterials.2013.06.061.
91. Bolshakov, I.N.; Svetlakov, A.V.; Sheina, Yu.I. Experimental partial and complete transsection of the spinal cord and its bioengineering reconstruction with chitosan-based substrates /Ed: K.G.Skryabin, S.N.Mikhailov, V.P.Varlamov. Chitosan, 2013, 593 p. Moscow. Center "Bioengineering" RAS (489-530).
92. Tiğli, R. S.; Gumüşderelioğlu, M. Evaluation of alginate-chitosan semi IPNs as cartilage scaffolds. J. Mater. Sci. Mater. Med. **2009**, 20 (3), 699–709; DOI: 10.1007/s10856-008-3624-x.
93. Matricardi, P.; Di Meo, C.; Coviello, T.; Hennink, W. E.; Alhaique, F. Interpenetrating polymer networks polysaccharide hydrogels for drug delivery and tissue engineering. Adv. Drug Deliv. Rev. **2013**, 65 (9), 1172–1187; DOI: 10.1016/j.addr.2013.04.002.
94. Venkatesan, J.; Bhatnagar, I.; Manivasagan, P.; Kang, K.-H.; Kim, S.-K. Alginate composites for bone tissue engineering: A review. Int. J. Biol. Macromol. **2015**, 72, 269-281; DOI: 10.1016/j.ijbiomac.2014.07.008.
95. Chung, T.-W.; Liu, D.-Z.; Wang, S.-Y.; Wang, S.-S. Enhancement of the growth of human endothelial cells by surface roughness at nanometer scale. Biomaterials. **2003**, 24 (25), 4655-4661; DOI: 10.1016/s0142-9612(03)00361-2.
96. Shchipunov, Y. A.; Postnova, I. Formation of calcium alginate-based macroporous materials comprising chitosan and hydroxyapatite. Colloid J. **2011**, 73 (4), 565–574; DOI:10.1134/S1061933X11040132.
97. Sharma, C.; Dinda, A. K.; Potdar, P. D.; Chou, C.-F.; Mishra, N. C. Fabrication and characterization of novel nano-biocomposite scaffold of chitosan–gelatin–alginate–hydroxyapatite for bone tissue engineering. Mater. Sci. Eng. C Mater. Biol. Appl. **2016**, 64, 416-427; DOI: 10.1016/j.msec.2016.03.060.
98. Jin, H.-H.; Lee, C.-H.; Lee, W.-K.; Lee, J.-K.; Park, H.-C.; Yoon, S.-Y. In-situ formation of the hydroxyapatite/chitosan-alginate composite scaffolds. Mater. Lett. **2008**, 62 (10), 1630–1633; DOI:10.1016/j.matlet.2007.09.043.
99. Liu, D.; Liu, Z.; Zou, J.; Li, L.; Sui, X.; Wang, B.; Yang, N.; Wang, B. Synthesis and characterization of a hydroxyapatite-sodium alginate-chitosan scaffold for bone regeneration. Front. Mater. **2021**, 8, 69; DOI:10.3389/fmats.2021.648980.
100. Park, J. S.; Choi, S. H.; Moon, I. S.; Cho, K. S.; Chai, J. K.; Kim, C. K. Eight-week histological analysis on the effect of chitosan on surgically created one-wall intrabony defects in beagle dogs. J. Clin. Periodontol. **2003**, 30 (5), 443–453; DOI: 10.1034/j.1600-051X.2003.10283.x.

Disclaimer/Publisher's Note: The statements, opinions and data contained in all publications are solely those of the individual author(s) and contributor(s) and not of MDPI and/or the editor(s). MDPI and/or the editor(s)

Preprints (www.preprints.org) | NOT PEER-REVIEWED | Posted: 16 August 2023 doi:10.20944/preprints202308.1140.v1

disclaim responsibility for any injury to people or property resulting from any ideas, methods, instructions or products referred to in the content.